vaccines. However, the C proteins of some vaccine strains remain fully functional. Nakatsu et al [47] compared the activities of C proteins from wild-type and vaccine strains using reverse-genetics techniques and found that a C protein identical to that of Zagreb equally regulated viral RNA synthesis, compared with the wild-type C protein, and was capable of circumventing the host IFN induction. Clearly, impaired function of the C protein is not a prerequisite to attenuation. The Ala73Val substitution is shared by all vaccine strains, including those derived from non-Edmonston progenitors. However, wild-type viruses from genotypes B3 and D3 also have Val at this position [132], making it less likely that the substitution has consequences for attenuation.

The role of the P/V/C gene in attenuation is well documented with different animal models. Recombinant viruses that do not express a V or a C protein are attenuated in rhesus macaques [139, 141]. A CEF-adapted virus with mutations affecting the P, V and C proteins as well as a substitution in M did not cause rash in macaques [127]. Takeda et al [142] showed that a recombinant MeV possessing the P gene of the Edmonston-tag strain exhibited attenuated gene expression levels in both cultured cells and mice expressing the hSLAM receptor. In cotton rats, recombinant viruses carrying the temperature-sensitive P gene of AIK-C were unable to replicate after intranasal inoculation [143].

The M gene has 50 cumulative changes in only 1008 nucleotides, of which 39 (78%) are coding changes, indicating both a higher overall substitution rate and a higher proportion of coding changes than the N, F, or L genes (Supplemental Table 1). Tahara et al [144] showed that the M protein derived from the wild-type IC-B strain associated with the cytoplasmic tail of the F protein, but it associated poorly with the cytoplasmic tail of the H protein. They further indicated that Pro64Ser and Glu89Lys substitutions allow a strong interaction of the M protein with the cytoplasmic tail of the H protein [144]. All measles vaccines with published sequence data possess the Glu89Lys substitutions in the M protein. The independently derived CAM-70 vaccine shares the Pro64Ser substitution with the Edmonston-derived Rubeovax, Moraten, and Schwarz, indicating the importance of this change. Vero cells do not efficiently express entry receptors for wild-type MeV. These substitutions allow wild-type MeV to grow well in Vero cells, presumably by enhancing MeV assembly and subsequent infectious particle production [144]. On the other hand, Pro64Ser and Glu89Lys inhibit receptor-dependent cell-cell fusion, thereby reducing virus growth in hSLAM-positive cells [145]. These data indicate that the Pro64Ser and Glu89Lys substitutions modulate the mode of MeV growth for adaptation to grow in different cell types. However, the contribution of the substitution at amino acid 89 to attenuation is unclear, because a wild-type MeV with the Glu89Lys substitution grew to higher titers in cotton rats than did the wild-type. [146]. In addition to the Glu89Lys substitution, all vaccine strains share a Gly61Asp substitution that is close to the important position of amino acid 64; however, no functional consequence is known for this substitution.

The F glycoprotein F is more conserved than the M or H genes, and the proportion of coding changes is lower (61%) (Supplemental Table 1). There are few differences between the F proteins of the prototype Edmonston strain and current wild-type strains [130, 131]. Importantly, the amino acid sequence of the F protein of the attenuated Zagreb strain is identical to the Edmonston wild-type F protein, indicating that large numbers of passages in various cell culture systems did not lead to adaptive changes. Furthermore, the Zagreb F protein is identical to the more recent wild-type IC-B isolate, a well-characterized virulent strain [131]. This demonstrates the high level of conservation in the F protein. One reported amino acid substitution that affects F protein function is Met94Val. F proteins possessing the Met94Val substitution exhibit enhanced cell-cell fusion activity [147–149]; however, Edmonston wild-type and all vaccine strains share the Met at this position. Edmonston-derived vaccines AIK-C, Schwarz, Moraten, and Rubeovax share a Ser362-Tyr substitution, whereas the independently derived CAM-70 has a Ser362Phe substitution. That the same position was changed in independently derived vaccine strains through different nucleotide substitutions may indicate the importance of this residue. Not surprisingly, important functional domains and motifs, such as the cytoplasmic tail, cleavage site, and fusion peptide, are completely conserved.

Similar to the M gene, the H gene has a very high ratio of coding changes (92%), indicating that these may be driven by selection. A large body of research is available for the study of receptor binding by measles H proteins [65]. Not surprisingly, all amino acid positions that are involved in binding to hSLAM and EpiR are conserved in Edmonston wild-type and all vaccine strains [72, 74, 150, 151]. Several amino acid positions that are involved in the ability of MeV strains to use CD46 have been reported [152–158]. Among these, the Asn481Tyr substitution is critical for use of CD46 as a receptor [152–154, 158–162]. The H proteins of all vaccine strains possess the Asn481Tyr substitution. However, this substitution alone does not confer efficient use of the CD46 receptor [163]. Tahara et al [164] showed that a Glu492Gly or Thr484Asn substitution, when present together with Asn481Tyr, enhances the ability of the wild-type H protein to use CD46. AIK-C, Zagreb, Leningrad-4, Shanghai-191, and Changchun-47 possess Thr484Asn, presumably enhancing their ability to bind CD46. Independently of Asn481Tyr, a Ser546Gly substitution can confer on MeV the ability to use CD46 as a receptor, and some Vero cell-grown MeV strains have the Ser546Gly substitution in their H proteins, instead of Asn481Tyr [129, 143, 156, 159, 160, 165–170]. The H protein of the Zagreb vaccine strain possesses Ser546Gly; however, so does the Edmonston wild-type. A recent study of the crystal structure of an MeV H protein complexed with CD46 also indicated critical roles of Asn481Tyr and Ser546Gly [151].

Interestingly, the Asn481Tyr substitution that is critical for using CD46 also promotes MeV infection of polarized epithelial cells via a CD46-independent pathway [74]. Therefore, all vaccine strains which possess Asn481Tyr in their H proteins may be able to use EpiR more efficiently than can wild-type MeV strains. A Val451 has been reported to improve CD46 binding, and all vaccine strains and the Edmonston wild-type strain share this amino acid. The fact that the Edmonston wild-type strain possesses amino acids corresponding to the cell culture–adapted phenotype may be evidence of some degree of cell culture adaptation. A Gly211 was reported to be involved in CD46 receptor down-regulation [152]. All vaccines share Gly211, in contrast to the Edmonston wild-type strain, which has a non–down-regulating Ser211. Receptor down regulation may be associated with protection of the infected cell from complement lysis [171]. In total, there are 3 amino acid substitutions in the H protein that are shared by all vaccine strains (amino acids 46, 211, and 481) and 1 additional substitution shared by all but the Zagreb strain (amino acid 546). Three of these 4 positions may play a role in CD46 binding or down-regulation, demonstrating the importance of receptor adaptation for growth of vaccines in hSLAM-negative cell lines. The functional consequence of the nonconservative Ser46Phe, which is located in the hydrophobic transmembrane domain [172], is unknown. The H proteins of some currently circulating wild-type strains have an additional glycosylation site, owing to an Asp416Asn substitution [62, 169, 173]. Although the glycosylation site at this position is located on the opposite side to the CD46-binding region [174], it has also been shown to modulate the CD46-binding activity of the H protein [164]. However, none of the vaccine strains possess this substitution. The cytoplasmic tails of the H proteins (amino acids 1-34) are completely conserved.

Considering its large size, the L gene is considerably more conserved than the other genes, with only 75 cumulative changes in 6549 nucleotides, of which only 36 (48%) are coding changes (Supplemental Table 1). This observation is consistent with previous analyses [96, 175]. The conservation of the L gene demonstrates that substitutions in the polymerase are deleterious for the virus and therefore not tolerated. On the basis of sequence conservation, 6 domains have been characterized for the L proteins of paramyxoviruses [83]. Eleven of the 16 positions that vary among the vaccine strains are located between the conserved domains, and 10 of these affect residues that are not conserved among the polymerases of nonsegmented negative strand viruses [81]. Of the 5 substitutions that affect residues within conserved domains, 3 affect residues that are conserved among polymerases. Ile235Val lies in a highly conserved hydrophobic stretch in domain I; however, it is a substitution that conserves the hydrophobic nature of the residue. Aside from this substitution, all highly conserved stretches and motifs [81] are completely conserved. One substitution (Asp1717Ala) is shared by all vaccine strains; however, several other wild-type strains in genotype A also have an Ala at this position [175]. Therefore, this is more likely to be a genotype-specific residue with Edmonston wild-type being the exception. Amino acids 1-408 of L are involved in L oligomerization, and hydrophobic amino acids between positions 25 and 339 are involved in binding to the P protein [82]. Four residues in this region are variable between vaccine L proteins, and 3 of these substitutions affect CAM-70 (Supplemental Table 1). Because interactions between the components of the polymerase complex are essential for virus replication, clearly these substitutions cannot inhibit L-L or L-P interactions. Whether they have subtle effects on these interactions is currently unknown. On the basis of investigations with recombinant MeV, the L gene of an attenuated laboratory strain contributed to the reduced gene expression and virus propagation in cell culture and in mice expressing hSLAM [142]. However, reduced gene expression was not observed when vaccine L proteins were used in a mini-replicon assay [142]. In addition, the L genes of measles vaccine strains showed higher activities than did the L genes of some wild-type MeV strains when analyzed by mini-replicon assays [176]. Therefore, the contribution of the L protein to attenuation remains unclear.

### Variability in Noncoding Regions

With 1 exception (nucleotide 7243, see below) all known cis-acting elements involved in transcription and replication (ie, promoter elements, intergenic regions, and gene-start and -end sequences) were conserved, as was the entire 37 nucleotide trailer sequence [2, 177]. The high level of conservation of trailer sequences of vaccine strains and wild-type viruses of different genotypes had already been reported [178]. Two nucleotide changes (26 and 42) in the leader sequence distinguish Edmonston wild-type from all vaccine strains. Although all vaccines share the A→T change at nucleotide 26, the substitution at nucleotide 42 is A→C for all vaccines except Zagreb, which has an A→T substitution. These positions affected transcription of a reporter gene in a mini-genome assay [178], and it is conceivable that they may affect replication of vaccine viruses. However, Liu et al [178] also reported that wild-type MeV isolates of genotype A had the same substitutions as the vaccine strains, so the relevance of these positions for attenuation is still unclear. In addition, no effect was observed when these substitutions were introduced into the infectious virus genome [142]. A substitution in Moraten, Schwarz, Rubeovax, and CAM-70 at nucleotide 1806 immediately precedes the AUG start codon of the P protein, possibly affecting translation efficiency [179]. It is intriguing that this substitution was selected for in Edmonston-derived and independently derived vaccines. However, the context of all MeV P start codons deviates from the optimal Kozak sequence [179], making it difficult to assess the effect of the substitution at nucleotide 1806. The suboptimal Kozak context of the P ORF possibly serves to enhance initiation at the downstream start codon for the overlapping C ORF, and it

is conceivable that substitutions that alter P protein translation could affect C protein translation.

Forty-eight nucleotide changes (affecting 19 positions) were located in the long untranslated region spanning the end of the M and the beginning of the F gene (Supplemental Table 1). The fact that MeV, like other morbilliviruses [56, 87], maintains this noncoding region of ~1 kB indicates that this region may play an important role, but its function is still unclear. It is possible that substitutions to this region may affect mRNA structure or stability. Changes to the long untranslated 3′ region of the M gene can increase M protein expression [89]. Deletion of the F nontranslated region reduced viral replication in a SCID mouse model [90] and nucleotide changes in this region decreased F protein expression [89]. Although the implications of single nucleotide changes in the F 5′ noncoding region are unclear, it is intriguing that 3 positions (4978, 5073, and 5349) in this region are changed in all vaccine strains, including those derived from non-Edmonston progenitors.

The only substitution that affects a conserved motif is a substitution in the gene-end signal of the F gene of Moraten and Schwarz (nucleotide 7243). However, although this nucleotide is part of the gene-end motif, this particular position is not conserved among the gene-end signals of MeV [95], making it less likely that the substitution changes transcription.

### Substitutions That Affect Most Vaccine Strains

Nucleotide substitutions, whether silent or not, that affect most vaccine strains are particularly interesting candidates for attenuation markers, especially if they are shared between Edmonston-derived and independently derived strains. There are 17 such changes among the vaccine strains analyzed to date (Table 1): 16 that affect all vaccine strains, and 1 (amino acid 546 in the H protein) that affects all vaccines except Zagreb. Three of these are silent nucleotide changes in coding sequences (nucleotides 4232, 5514, and 14579). Five affect noncoding regions (nucleotides 26, 42, 4978, 5073, and 5349), whereas the remaining 9 predict coding changes in P, V, C, M, H, and L proteins. Several of these substitutions have demonstrated functional consequences, at least in in vitro systems, including nucleotides 26 and 42 as well as amino acids 89 in the M protein and amino acids 211, 481, and 546 in the H protein. However, functional consequences of these substitutions could not always be confirmed in animal models [142, 146]. Because attenuation is generally assumed to be the result of an accumulation of mutations, it is possible that introduction of 1 or a few changes at a time will not be sufficient to produce measurable differences in pathogenicity in animal models.

## GENETIC STABILITY OF VACCINE SEQUENCES IN CELL CULTURE AND VACCINEES

Borges et al [97] sequenced CAM-70 directly from the seed lot and after 10 passages in primary chicken embryo fibroblasts and found complete sequence identity. Baricevic et al [180] compared a master seed lot of Zagreb with a working seed and also found complete sequence identity. However, 6 nucleotide differences were found between their sequence and the sequence of Zagreb, as published by Parks et al [96, 97], that is used in this review [180]. Passages of the vaccines in the laboratories where they were used may account for those differences. Sequences derived from vaccine-associated measles cases usually only report the carboxyl-terminal region of the N protein which was chosen for genotype analysis. Analysis of 7 such sequences available on GenBank revealed complete nucleotide identity with Moraten/Schwarz (B. Bankamp, unpublished data).

## SUBGENOMIC RNAs

Defective interfering particles (DIs) have been found in several vaccine strains, including Zagreb, AIK-C, and CAM-70 [181, 182]. DIs contain subgenomic RNAs which are generated during replication of the full-length genome [183]. Because of large deletions in the protein coding regions, they require coinfection of the cell with a full-length genome to provide viral proteins. DIs can interfere with the replication of the full-length genome, leading to reduced viral titers in cell culture [184]. Viral stocks that contain DIs induce higher amounts of IFN [185]. Whether the presence of DIs or the resulting increase in IFN induction play any role in attenuation is not known.

## IMMUNOGENICITY, PROTECTION AGAINST DIFFERENT GENOTYPES, AND ADVERSE EVENTS

Measles vaccine is one of the most efficacious vaccines presently available [113]. Seroconversion rates have exceeded 98% in children aged ≥12 months for most vaccines studied [9, 103, 114–116, 186, 187]. These data lead to the conclusion that there are no significant differences between seroconversion rates of the different vaccine strains.

On the basis of the sequences of their N and H genes, MeVs can be assigned to 1 of 23 genotypes and 1 provisional genotype [11, 12]. All vaccine strains and their wild-type progenitors are assigned to genotype A. Experiments with monoclonal antibodies have defined antigenic differences between the H proteins of genotype A vaccines and the H proteins of wild-type viruses grouped in other genotypes [62, 188, 189]. However, there is only 1 serotype for measles, and serum samples from vaccinees neutralize viruses from a wide range of genotypes, albeit with different neutralization titers [188, 190] More importantly, despite the presence of different endemic genotypes, vaccination programs with standard measles vaccines have been successful in every country where they were performed adequately [191–193]. Suboptimal seroconversion after vaccination is likely the result of inadequate coverage; improper administration, transport, or storage of vaccine; or age of the vaccine recipients [194–196].

Measles vaccines have an outstanding safety record, with only very small numbers of adverse events reported. The most common adverse events are fever and rash beginning 8-12 days after vaccination. Most of these reactions resolve quickly without need of clinical intervention [113]. The insufficiently attenuated Leningrad-4 caused fever (temperature, >38.7°C) and rash in all 7 vaccine recipients [114], and Rubeovax caused fever (temperature, >38.2°C) in 46% of recipients and rash in 16% of cases [9]. The further-attenuated strains induced less severe and less frequent side effects, from 2% of vaccinees that presented with fever (temperature, >38°C) after vaccination with Zagreb to 21% of subjects with temperatures >38.2°C after vaccination with Schwarz [9, 103, 105, 114–116, 187, 197]. The occurrence of rash ranges from 3% in Moraten-vaccinees to 20% in AIK-C-vaccinees [9, 103, 116, 187, 198, 199]. Although there appear to be significant differences in the rates of rash and fever, most vaccines were tested in separate studies and under different conditions, and the cutoff values for fever varied from study to study. Vaccines can cause severe adverse events in immunocompromised individuals whose immune systems are incapable of clearing the virus [200–202]. Children who are human immunodeficiency virus seropositive but do not demonstrate immune impairment can be safely vaccinated with measles vaccine, and they derive some protection from wild-type virus [203, 204]. There is no evidence that measles vaccines are responsible for SSPE [205], because only wild-type viruses have been detected in these cases.

## GENETIC BASIS FOR ATTENUATION

Attenuation is the result of adaptation of the virus to growth conditions in nonpermissive cell culture, in the case of measles especially avian cell lines. This scenario implies that many attenuating mutations affect interactions with host cell proteins. Presumably such mutations increase interaction with cellular proteins in avian cells yet reduce the ability of the protein to carry out its functions in its human host. Most experiments have relied on mammalian cells for the analysis of differences between wild-type and vaccine viruses, whereas few studies used avian cells [127, 206, 207]. Substitutions in the P, V, C, M, and H proteins have been most often associated with measurable differences between vaccine strains and wild-type strains. Specifically, receptor use and interactions with IFN induction/signaling have been shown to be important, as well as substitutions in the M protein that affect interactions with the nucleocapsid. The L proteins of vaccine viruses also appear to contribute to attenuation in ways that are not yet understood. However, no common functional change that affects all vaccines has been demonstrated. This may be because multiple, cumulative changes appear to be responsible for attenuation and because separate passage histories may have given each vaccine strain a different pathway to attenuation. Therefore, although we have made significant progress in analyzing functional differences between wild-type and vaccine viruses, the molecular basis of attenuation remains unknown. Almost every gene contributes in some way to a cell culture-adapted phenotype; this complicates the identification of the molecular basis for attenuation in humans. Recombination, which is an efficient means for rapid genetic change for many viruses, does not occur in paramyxoviruses. No recombinant viruses have been isolated from natural infections. One constraint that may explain the absence of recombination is the rule of 6 [85, 208]. Genome lengths in the subfamily *Paramyxovirinae* have to be evenly divisible by 6, and genomes with insertions or deletions that violate the rule of 6 would result in nonviable virus. The complex pathway to cell culture adaptation and, ultimately, attenuation together with the absence of recombination suggest that it would be extremely unlikely for measles vaccine strains to revert to a virulent phenotype.

## Supplementary Data

Supplementary data are available at *The Journal of Infectious Diseases* online.

## Funding

No external funds were used at the US Centers for Disease Control and Prevention; the National Institute of Infectious Diseases, Japan; or the National Institute for Viral Disease Control and Prevention, China.

## References

1. Hilleman MR. Current overview of the pathogenesis and prophylaxis of measles with focus on practical implications. Vaccine **2001**; 20:651–65.
2. Griffin DA. Measles virus. In: Fields BN, Knipe DM, Howley PM, eds. Fields Virology. 5th ed. Vol 2. Philadelphia: Wolters Kluwer Health/ Lippincott Williams & Wilkins, **2007**; 1551–85.
3. Moss WJ, Griffin DE. Global measles elimination. Nat Rev Microbiol **2006**; 4:900–8.
4. Schneider-Schaulies J, Meulen V, Schneider-Schaulies S. Measles infection of the central nervous system. J Neurovirol **2003**; 9:247–52.
5. Measles-Initiative. WHO/UNICEF joint annual measles report 2009, 2010. http://measlesinitiative.org. Accessed 14 March 2011.
6. Wolfson LJ, Strebel PM, Gacic-Dobo M, Hoekstra EJ, McFarland JW, Hersh BS. Has the 2005 measles mortality reduction goal been achieved? A natural history modelling study. Lancet **2007**; 369:191–200.
7. Enders JF, Peebles TC. Propagation in tissue cultures of cytopathogenic agents from patients with measles. Proc Soc Exp Biol Med **1954**; 86:277–86.
8. Rota JS, Wang ZD, Rota PA, Bellini WJ. Comparison of sequences of the H, F, and N coding genes of measles virus vaccine strains. Virus Res **1994**; 31:317–30.
9. Hilleman MR, Buynak EB, Weibel RE, Stokes J Jr, Whitman JE Jr, Leagus MB. Development and evaluation of the Moraten measles virus vaccine. JAMA **1968**; 206:587–90.
10. Atkinson W, Wolfe S, Hamborsky J, McIntyre L;. Centers for Disease Control and Prevention. Epidemiology and prevention of vaccine-preventable diseases. 11th ed. Washington, DC: Public Health Foundation, 2009.

11. WHO. Nomenclature for describing the genetic characteristics of wild-type measles viruses (update). Wkly Epidemiol Rec **2001**; 76:249–51.
12. Zhang Y, Ding Z, Wang H, et al. New measles virus genotype associated with outbreak, China. Emerg Infect Dis **2010**; 16:943–7.
13. Riddell MA, Rota JS, Rota PA. Review of the temporal and geographical distribution of measles virus genotypes in the prevaccine and postvaccine eras. Virol J **2005**; 2:87.
14. Bellini WJ, Englund G, Rozenblatt S, Arnheiter H, Richardson CD. Measles virus P gene codes for two proteins. J Virol **1985**; 53:908–19.
15. Cattaneo R, Kaelin K, Baczko K, Billeter MA. Measles virus editing provides an additional cysteine-rich protein. Cell **1989**; 56:759–64.
16. Longhi S, Receveur-Brechot V, Karlin D, et al. The C-terminal domain of the measles virus nucleoprotein is intrinsically disordered and folds upon binding to the C-terminal moiety of the phosphoprotein. J Biol Chem **2003**; 278:18638–48.
17. Rota PA, Featherstone DA, Bellini WJ. Molecular epidemiology of measles virus. Curr Top Microbiol Immunol **2009**; 330:129–50.
18. Taylor MJ, Godfrey E, Baczko K, ter Meulen V, Wild TF, Rima BK. Identification of several different lineages of measles virus. J Gen Virol **1991**; 72:83–8.
19. Bankamp B, Horikami SM, Thompson PD, Huber M, Billeter M, Moyer SA. Domains of the measles virus N protein required for binding to P protein and self-assembly. Virology **1996**; 216:272–7.
20. Harty RN, Palese P. Measles virus phosphoprotein (P) requires the NH2- and COOH-terminal domains for interactions with the nucleoprotein (N) but only the COOH terminus for interactions with itself. J Gen Virol **1995**; 76:2863–7.
21. Iwasaki M, Takeda M, Shirogane Y, Nakatsu Y, Nakamura T, Yanagi Y. The matrix protein of measles virus regulates viral RNA synthesis and assembly by interacting with the nucleocapsid protein. J Virol **2009**; 83:10374–83.
22. Laine D, Trescol-Biemont MC, Longhi S, et al. Measles virus (MV) nucleoprotein binds to a novel cell surface receptor distinct from FcγRII via its C-terminal domain: role in MV-induced immunosuppression. J Virol **2003**; 77:11332–46.
23. Sato H, Masuda M, Kanai M, Tsukiyama-Kohara K, Yoneda M, Kai C. Measles virus N protein inhibits host translation by binding to eIF3-p40. J Virol **2007**; 81:11569–76.
24. tenOever BR. Servant MJ, Grandvaux N, Lin R, Hiscott J. Recognition of the measles virus nucleocapsid as a mechanism of IRF-3 activation. J Virol **2002**; 76:3659–69.
25. Zhang X, Glendening C, Linke H, et al. Identification and characterization of a regulatory domain on the carboxyl terminus of the measles virus nucleocapsid protein. J Virol **2002**; 76:8737–46.
26. Parks CL, Lerch RA, Walpita P, Sidhu MS, Udem SA. Enhanced measles virus cDNA rescue and gene expression after heat shock. J Virol **1999**; 73:3560–6.
27. Vasconcelos DY, Cai XH, Oglesbee MJ. Constitutive overexpression of the major inducible 70 kDa heat shock protein mediates large plaque formation by measles virus. J Gen Virol **1998**; 79:2239–47.
28. Zhang X, Bourhis JM, Longhi S, et al. Hsp72 recognizes a P binding motif in the measles virus N protein C-terminus. Virology **2005**; 337:162–74.
29. Carsillo T, Zhang X, Vasconcelos D, Niewiesk S, Oglesbee M. A single codon in the nucleocapsid protein C terminus contributes to in vitro and in vivo fitness of Edmonston measles virus. J Virol **2006**; 80:2904–12.
30. Liston P, DiFlumeri C, Briedis DJ. Protein interactions entered into by the measles virus P, V, and C proteins. Virus Res **1995**; 38:241–59.
31. Sedlmeier R, Neubert WJ. The replicative complex of paramyxoviruses: structure and function. Adv Virus Res **1998**; 50:101–39.
32. Curran J, Marq JB, Kolakofsky D. An N-terminal domain of the Sendai paramyxovirus P protein acts as a chaperone for the NP protein during the nascent chain assembly step of genome replication. J Virol **1995**; 69:849–55.
33. Fontana JM, Bankamp B, Rota PA. Inhibition of interferon induction and signaling by paramyxoviruses. Immunol Rev **2008**; 225:46–67.
34. Caignard G, Guerbois M, Labernardiere JL, et al. Measles virus V protein blocks Jak1-mediated phosphorylation of STAT1 to escape IFN-alpha/beta signaling. Virology **2007**; 368:351–62.
35. Nakatsu Y, Takeda M, Ohno S, Koga R, Yanagi Y. Translational inhibition and increased interferon induction in cells infected with C protein-deficient measles virus. J Virol **2006**; 80:11861–7.
36. Ohno S, Ono N, Takeda M, Takeuchi K, Yanagi Y. Dissection of measles virus V protein in relation to its ability to block alpha/beta interferon signal transduction. J Gen Virol **2004**; 85:2991–9.
37. Palosaari H, Parisien JP, Rodriguez JJ, Ulane CM, Horvath CM. STAT protein interference and suppression of cytokine signal transduction by measles virus V protein. J Virol **2003**; 77:7635–44.
38. Ramachandran A, Parisien JP, Horvath CM. STAT2 is a primary target for measles virus V protein-mediated alpha/beta interferon signaling inhibition. J Virol **2008**; 82:8330–8.
39. Takeuchi K, Kadota SI, Takeda M, Miyajima N, Nagata K. Measles virus V protein blocks interferon (IFN)-alpha/beta but not IFN-gamma signaling by inhibiting STAT1 and STAT2 phosphorylation. FEBS Lett **2003**; 545:177–82.
40. Childs K, Stock N, Ross C, et al. mda-5, But not RIG-I, is a common target for paramyxovirus V proteins. Virology **2007**; 359:190–200.
41. Ikegame S, Takeda M, Ohno S, Nakatsu Y, Nakanishi Y, Yanagi Y. Both RIG-I and MDA5 RNA helicases contribute to the induction of alpha/beta interferon in measles virus-infected human cells. J Virol **2010**; 84:372–9.
42. Nakatsu Y, Takeda M, Ohno S, Shirogane Y, Iwasaki M, Yanagi Y. Measles virus circumvents the host interferon response by different actions of the C and V proteins. J Virol **2008**; 82:8296–306.
43. Fontana JM, Bankamp B, Bellini WJ, Rota PA. Regulation of interferon signaling by the C and V proteins from attenuated and wild-type strains of measles virus. Virology **2008**; 374:71–81.
44. Shaffer JA, Bellini WJ, Rota PA. The C protein of measles virus inhibits the type I interferon response. Virology **2003**; 315:389–97.
45. Bankamp B, Wilson J, Bellini WJ, Rota PA. Identification of naturally occurring amino acid variations that affect the ability of the measles virus C protein to regulate genome replication and transcription. Virology **2005**; 336:120–9.
46. Reutter GL, Cortese-Grogan C, Wilson J, Moyer SA. Mutations in the measles virus C protein that up regulate viral RNA synthesis. Virology **2001**; 285:100–9.
47. Nakatsu Y, Takeda M, Iwasaki M, Yanagi Y. A highly attenuated measles virus vaccine strain encodes a fully functional C protein. J Virol **2009**; 83:11996–2001.
48. Witko SE, Kotash C, Sidhu MS, Udem SA, Parks CL. Inhibition of measles virus minireplicon-encoded reporter gene expression by V protein. Virology **2006**; 348:107–19.
49. Parks CL, Witko SE, Kotash C, Lin SL, Sidhu MS, Udem SA. Role of V protein RNA binding in inhibition of measles virus minigenome replication. Virology **2006**; 348:96–106.
50. Wild TF, Buckland R. Functional aspects of envelope-associated measles virus proteins. Curr Top Microbiol Immunol **1995**; 191:51–64.
51. Cathomen T, Mrkic B, Spehner D, et al. A matrix-less measles virus is infectious and elicits extensive cell fusion: consequences for propagation in the brain. EMBO J **1998**; 17:3899–908.
52. Cathomen T, Naim HY, Cattaneo R. Measles viruses with altered envelope protein cytoplasmic tails gain cell fusion competence. J Virol **1998**; 72:1224–34.
53. Spielhofer P, Bachi T, Fehr T, et al. Chimeric measles viruses with a foreign envelope. J Virol **1998**; 72:2150–9.
54. Hirano A, Ayata M, Wang AH, Wong TC. Functional analysis of matrix proteins expressed from cloned genes of measles virus variants that cause subacute sclerosing panencephalitis reveals a common defect in nucleocapsid binding. J Virol **1993**; 67:1848–53.

55. Suryanarayana K, Baczko K, ter Meulen V, Wagner RR. Transcription inhibition and other properties of matrix proteins expressed by M genes cloned from measles viruses and diseased human brain tissue. J Virol **1994**; 68:1532–43.
56. Richardson C, Hull D, Greer P, et al. The nucleotide sequence of the mRNA encoding the fusion protein of measles virus (Edmonston strain): a comparison of fusion proteins from several different paramyxoviruses. Virology **1986**; 155:508–23.
57. Alkhatib G, Shen SH, Briedis D, et al. Functional analysis of N-linked glycosylation mutants of the measles virus fusion protein synthesized by recombinant vaccinia virus vectors. J Virol **1994**; 68:1522–31.
58. Richardson CD, Choppin PW. Oligopeptides that specifically inhibit membrane fusion by paramyxoviruses: studies on the site of action. Virology **1983**; 131:518–32.
59. Samuel O, Shai Y. Participation of two fusion peptides in measles virus-induced membrane fusion: emerging similarity with other paramyxoviruses. Biochemistry **2001**; 40:1340–9.
60. Buckland R, Gerald C, Barker R, Wild TF. Fusion glycoprotein of measles virus: nucleotide sequence of the gene and comparison with other paramyxoviruses. J Gen Virol **1987**; 68:1695–703.
61. Hu A, Cattaneo R, Schwartz S, Norrby E. Role of N-linked oligosaccharide chains in the processing and antigenicity of measles virus haemagglutinin protein. J Gen Virol **1994**; 75:1043–52.
62. Santibanez S, Niewiesk S, Heider A, et al. Probing neutralizing-antibody responses against emerging measles viruses (MVs): immune selection of MV by H protein-specific antibodies? J Gen Virol **2005**; 86:365–74.
63. Moll M, Klenk HD, Herrler G, Maisner A. A single amino acid change in the cytoplasmic domains of measles virus glycoproteins H and F alters targeting, endocytosis, and cell fusion in polarized Madin-Darby canine kidney cells. J Biol Chem **2001**; 276:17887–94.
64. Naim HY, Ehler E, Billeter MA. Measles virus matrix protein specifies apical virus release and glycoprotein sorting in epithelial cells. EMBO J **2000**; 19:3576–85.
65. Yanagi Y, Takeda M, Ohno S, Hashiguchi T. Measles virus receptors. Curr Top Microbiol Immunol **2009**; 329:13–30.
66. Tatsuo H, Ono N, Tanaka K, Yanagi Y. SLAM. (CDw150) is a cellular receptor for measles virus. Nature **2000**; 406:893–7.
67. Dorig RE, Marcil A, Chopra A, Richardson CD. The human CD46 molecule is a receptor for measles virus (Edmonston strain). Cell **1993**; 75:295–305.
68. Naniche D, Varior-Krishnan G, Cervoni F, et al. Human membrane cofactor protein (CD46) acts as a cellular receptor for measles virus. J Virol **1993**; 67:6025–32.
69. Aversa G, Chang CC, Carballido JM, Cocks BG, de Vries JE. Engagement of the signaling lymphocytic activation molecule (SLAM) on activated T cells results in IL-2-independent, cyclosporin A-sensitive T cell proliferation and IFN-gamma production. J Immunol **1997**; 158:4036–44.
70. Cocks BG, Chang CC, Carballido JM, Yssel H, de Vries JE, Aversa G. A novel receptor involved in T-cell activation. Nature **1995**; 376:260–3.
71. Sidorenko SP, Clark EA. Characterization of a cell surface glycoprotein IPO-3, expressed on activated human B and T lymphocytes. J Immunol **1993**; 151:4614–24.
72. Leonard VH, Sinn PL, Hodge G, et al. Measles virus blind to its epithelial cell receptor remains virulent in rhesus monkeys but cannot cross the airway epithelium and is not shed. J Clin Invest **2008**; 118:2448–58.
73. Shirogane Y, Takeda M, Tahara M, Ikegame S, Nakamura T, Yanagi Y. Epithelial-mesenchymal transition abolishes the susceptibility of polarized epithelial cell lines to measles virus. J Biol Chem **2010**; 285:20882–90.
74. Tahara M, Takeda M, Shirogane Y, Hashiguchi T, Ohno S, Yanagi Y. Measles virus infects both polarized epithelial and immune cells by using distinctive receptor-binding sites on its hemagglutinin. J Virol **2008**; 82:4630–7.
75. Takeda M. Measles virus breaks through epithelial cell barriers to achieve transmission. J Clin Invest **2008**; 118:2386–9.
76. Takeda M, Tahara M, Hashiguchi T, et al. A human lung carcinoma cell line supports efficient measles virus growth and syncytium formation via a SLAM- and CD46-independent mechanism. J Virol **2007**; 81:12091–6.
77. de Swart RL, Yuksel S, Osterhaus AD. Relative contributions of measles virus hemagglutinin- and fusion protein-specific serum antibodies to virus neutralization. J Virol **2005**; 79:11547–51.
78. Grdzelishvili VZ, Smallwood S, Tower D, Hall RL, Hunt DM, Moyer SA. A single amino acid change in the L-polymerase protein of vesicular stomatitis virus completely abolishes viral mRNA cap methylation. J Virol **2005**; 79:7327–37.
79. Hercyk N, Horikami SM, Moyer SA. The vesicular stomatitis virus L protein possesses the mRNA methyltransferase activities. Virology **1988**; 163:222–5.
80. Ogino T, Kobayashi M, Iwama M, Mizumoto K. Sendai virus RNA-dependent RNA polymerase L protein catalyzes cap methylation of virus-specific mRNA. J Biol Chem **2005**; 280:4429–35.
81. Poch O, Blumberg BM, Bougueleret L, Tordo N. Sequence comparison of five polymerases (L proteins) of unsegmented negative-strand RNA viruses: theoretical assignment of functional domains. J Gen Virol **1990**; 71:1153–62.
82. Cevik B, Holmes DE, Vrotsos E, Feller JA, Smallwood S, Moyer SA. The phosphoprotein (P) and L binding sites reside in the N-terminus of the L subunit of the measles virus RNA polymerase. Virology **2004**; 327:297–306.
83. Horikami SM, Smallwood S, Bankamp B, Moyer SA. An amino-proximal domain of the L protein binds to the P protein in the measles virus RNA polymerase complex. Virology **1994**; 205:540–5.
84. Radecke F, Spielhofer P, Schneider H, et al. Rescue of measles viruses from cloned DNA. EMBO J **1995**; 14:5773–84.
85. Sidhu MS, Chan J, Kaelin K, et al. Rescue of synthetic measles virus minireplicons: measles genomic termini direct efficient expression and propagation of a reporter gene. Virology **1995**; 208:800–7.
86. Crowley JC, Dowling PC, Menonna J, et al. Sequence variability and function of measles virus 3' and 5' ends and intercistronic regions. Virology **1988**; 164:498–506.
87. Bellini WJ, Englund G, Richardson CD, Rozenblatt S, Lazzarini RA. Matrix genes of measles virus and canine distemper virus: cloning, nucleotide sequences, and deduced amino acid sequences. J Virol **1986**; 58:408–16.
88. Cathomen T, Buchholz CJ, Spielhofer P, Cattaneo R. Preferential initiation at the second AUG of the measles virus F mRNA: a role for the long untranslated region. Virology **1995**; 214:628–32.
89. Takeda M, Ohno S, Seki F, Nakatsu Y, Tahara M, Yanagi Y. Long untranslated regions of the measles virus M and F genes control virus replication and cytopathogenicity. J Virol **2005**; 79:14346–54.
90. Valsamakis A, Schneider H, Auwaerter PG, Kaneshima H, Billeter MA, Griffin DE. Recombinant measles viruses with mutations in the C, V, or F gene have altered growth phenotypes in vivo. J Virol **1998**; 72:7754–61.
91. Lamb RA, Parks GD. Paramyxoviridae: the viruses and their replication. In: Fields BN, Knipe DM, Howley PM, eds. Fields Virology. 5th ed. Vol 1. Philadelphia: Wolters Kluwer Health/Lippincott Williams & Wilkins, **2007**; 1449–96.
92. Hall WW, Meulen V. Rolyadenylic acid [poly(A)] sequences associated with measles virus intracellular ribonucleic acid (RNA) species. J Gen Virol **1977**; 35:487–510.
93. Rima BK, Duprex WP. The measles virus replication cycle. Curr Top Microbiol Immunol **2009**; 329:77–102.
94. Mori T, Sasaki K, Hashimoto H, Makino S. Molecular cloning and complete nucleotide sequence of genomic RNA of the AIK-C strain of attenuated measles virus. Virus Genes **1993**; 7:67–81.
95. Parks CL, Lerch RA, Walpita P, Wang HP, Sidhu MS, Udem SA. Analysis of the noncoding regions of measles virus strains in the Edmonston vaccine lineage. J Virol **2001**; 75:921–33.
96. Parks CL, Lerch RA, Walpita P, Wang HP, Sidhu MS, Udem SA. Comparison of predicted amino acid sequences of measles virus strains in the Edmonston vaccine lineage. J Virol **2001**; 75:910–20.

97. Borges MB, Caride E, Jabor AV, et al. Study of the genetic stability of measles virus CAM-70 vaccine strain after serial passages in chicken embryo fibroblasts primary cultures. Virus Genes **2008**; 36:35–44.
98. Zhang Y, Zhou J, Bellini WJ, Xu W, Rota PA. Genetic characterization of Chinese measles vaccines by analysis of complete genomic sequences. J Med Virol **2009**; 81:1477–83.
99. Smorodintsev AA, Boichuk LM, Shikina ES, Batanova TB, Bystryakova LV, Peradze TV. Clinical and immunological response to live tissue culture vaccine against measles. Acta Virol **1960**; 4:201–4.
100. Ueda S, Takahashi M, Minekawa Y, Ogino T, Suzuki N. Studies on further attenuated live measles vaccine. I. Adaptation of measles virus to the chorioallantoic membrane of chick embryo and clinical tests on the strain. Biken J **1970**; 13:111–6.
101. Xiang JZ, Chen ZH. Measles vaccine in the People's Republic of China. Rev Infect Dis **1983**; 5:506–10.
102. Makino S. Development and characteristics of live AIK-C measles virus vaccine: a brief report. Rev Infect Dis **1983**; 5:504–5.
103. Makino S, Sasaki K, Nakamura N, Nakagawa M, Nakajima S. Studies on the modification of the live AIK measles vaccine. II. Development and evaluation of the live AIK-C measles vaccine. Kitasato Arch Exp Med **1974**; 47:13–21.
104. Ikic D, Beck M, Juzbasic M. Characterization of Edmonston-Zagreb measles virus. Proc. Symposium on Human Diploid Cells. Zagreb, Yugoslavia: Yugoslav Academy of Sciences and Arts, **1970**; 121–9.
105. Ikic D, Juzbasic M, Beck M, Hrabar A, Cimbur-Schreiber T. Attenuation and characterisation of Edmonston-Zagreb measles virus. Ann Immunol Hung **1972**; 16:175–81.
106. Tamura K, Dudley J, Nei M, Kumar S. MEGA4: Molecular Evolutionary Genetics Analysis (MEGA) software version 4.0. Mol Biol Evol **2007**; 24:1596–99.
107. Jayaraman KS. Biotech boom. Nature **2005**; 436:480–3.
108. Hilleman MR, Stokes J Jr, Buynak EB, Weibel R, Halenda R, Goldner H. Studies of live attenuated measles virus vaccine in man. II. Appraisal of efficacy. Am J Public Health Nations Health **1962**; 52:S44–56.
109. Katz SL, Enders JF, Holloway A. The development and evaluation of an attenuated measles virus vaccine. Am J Public Health Nations Health **1962**; 52:S5–10.
110. Stokes J Jr, Weibel R, Halenda R, Reilly CM, Hilleman MR. Enders' live measles-virus vaccine with human immune globulin. I. Clinical reactions. Am J Dis Child **1962**; 103:366–72.
111. Stokes J Jr, Weibel R, Halenda R, Reilly CM, Hilleman MR. Studies of live attenuated measles virus vaccine in man. I. Clinical aspects. Am J Public Health Nations Health **1962**; 52:S29–43.
112. Schwarz AJ. Preliminary tests of a highly attenuated measles vaccine. Am J Dis Child **1962**; 103:386–9.
113. Strebel PM, Papania MJ, Dayan GH, Halsey NA. Measles vaccine. In: Plotkin SA, Orenstein WA, Offit PA, eds. Vaccines. 5th ed. Philadelphia: Saunders, 2008: 353–98.
114. Huang CH, Chia PY, Chu FT, et al. Studies on attenuated measles vaccine. I. Clinical and immunologic response to measles virus attenuated in human amnion cells. Chin Med J **1962**; 81:9–14.
115. Chun H, T'Eh-chang H, Kuo-hua T, et al. Clinical and immunologic observations on two lines of attenuated measles vaccine virus upon passage in chick embryo cell culture. Chin Med J (Engl) **1975**; 1:283–6.
116. Okuno Y, Ueda S, Kurimura T, Suzuki N, Yamanishi K. Studies on further attenuated liver measles vaccine. VII. Development and evaluation of CAM-70 measles virus vaccine. Biken J **1971**; 14:253–8.
117. Takaku K, Sasada T, Konobe T, Onishi K, Ueda S. Studies on further attenuated live measles vaccine. 3. Selection of less reactive variants of CAM measles vaccine virus. Biken J **1970**; 13:163–8.
118. Kato S, Ohgimoto S, Sharma LB, et al. Reduced ability of hemagglutinin of the CAM-70 measles virus vaccine strain to use receptors CD46 and SLAM. Vaccine **2009**; 27:3838–48.
119. Smorodintsev AA, Boychuk LM, Shikina ES, et al. Prevention of measles by use of live vaccines in the U.S.S.R. Arch Gesamte Virusforsch **1965**; 16:284–93.
120. Smorodintsev AA, Boychuk LM, Shikina ES, et al. Further experiences with live measles vaccines in USSR: use of virus propagated in chick fibroblasts and in guinea pig kidney cells. Am J Dis Child **1962**; 103:384–6.
121. Korber B. HIV signature and sequence variation analysis. In: Rodrigo AG, Learn GH, eds. Computational analysis of HIV molecular sequences. Dordrecht, the Netherlands: Kluwer Academic Publishers, 2000: 55–72.
122. Rota PA, Bloom AE, Vanchiere JA, Bellini WJ. Evolution of the nucleoprotein and matrix genes of wild-type strains of measles virus isolated from recent epidemics. Virology **1994**; 198:724–30.
123. Cattaneo R, Schmid A, Eschle D, Baczko K, ter Meulen V, Billeter MA. Biased hypermutation and other genetic changes in defective measles viruses in human brain infections. Cell **1988**; 55:255–65.
124. Bass BL, Weintraub H, Cattaneo R, Billeter MA. Biased hypermutation of viral RNA genomes could be due to unwinding/modification of double-stranded RNA. Cell **1989**; 56:331.
125. Billeter MA, Cattaneo R, Spielhofer P, et al. Generation and properties of measles virus mutations typically associated with subacute sclerosing panencephalitis. Ann N Y Acad Sci **1994**; 724:367–77.
126. Bankamp B, Fontana JM, Bellini WJ, Rota PA. Adaptation to cell culture induces functional differences in measles virus proteins. Virol J **2008**; 5:129.
127. Bankamp B, Hodge G, McChesney MB, Bellini WJ, Rota PA. Genetic changes that affect the virulence of measles virus in a rhesus macaque model. Virology **2008**; 373:39–50.
128. Druelle J, Sellin CI, Waku-Kouomou D, Horvat B, Wild FT. Wild type measles virus attenuation independent of type I IFN. Virol J **2008**; 5:22.
129. Takeda M, Kato A, Kobune F, et al. Measles virus attenuation associated with transcriptional impediment and a few amino acid changes in the polymerase and accessory proteins. J Virol **1998**; 72:8690–6.
130. Takeda M, Sakaguchi T, Li Y, Kobune F, Kato A, Nagai Y. The genome nucleotide sequence of a contemporary wild strain of measles virus and its comparison with the classical Edmonston strain genome. Virology **1999**; 256:340–50.
131. Takeuchi K, Miyajima N, Kobune F, Tashiro M. Comparative nucleotide sequence analyses of the entire genomes of B95a cell-isolated and vero cell-isolated measles viruses from the same patient. Virus Genes **2000**; 20:253–7.
132. Bankamp B, Lopareva EN, Kremer JR, et al. Genetic variability and mRNA editing frequencies of the phosphoprotein genes of wild-type measles viruses. Virus Res **2008**; 135:298–306.
133. Devaux P, von Messling V, Songsungthong W, Springfeld C, Cattaneo R. Tyrosine 110 in the measles virus phosphoprotein is required to block STAT1 phosphorylation. Virology **2007**; 360:72–83.
134. Das T, Schuster A, Schneider-Schaulies S, Banerjee AK. Involvement of cellular casein kinase II in the phosphorylation of measles virus P protein: identification of phosphorylation sites. Virology **1995**; 211:218–26.
135. Fukuda A, Sugiura A. Temperature-dependent growth restriction in measles vaccine strains. Jpn J Med Sci Biol **1983**; 36:331–5.
136. Komase K, Nakayama T, Iijima M, Miki K, Kawanishi R, Uejima H. The phosphoprotein of attenuated measles AIK-C vaccine strain contributes to its temperature-sensitive phenotype. Vaccine **2006**; 24:826–34.
137. Devaux P, Cattaneo R. Measles virus phosphoprotein gene products: conformational flexibility of the P/V protein amino-terminal domain and C protein infectivity factor function. J Virol **2004**; 78:11632–40.
138. Patterson JB, Thomas D, Lewicki H, Billeter MA, Oldstone MB. V and C proteins of measles virus function as virulence factors in vivo. Virology **2000**; 267:80–9.
139. Takeuchi K, Takeda M, Miyajima N, et al. Stringent requirement for the C protein of wild-type measles virus for growth both in vitro and in macaques. J Virol **2005**; 79:7838–44.
140. Tober C, Seufert M, Schneider H, et al. Expression of measles virus V protein is associated with pathogenicity and control of viral RNA synthesis. J Virol **1998**; 72:8124–32.

141. Devaux P, Hodge G, McChesney MB, Cattaneo R. Attenuation of V- or C-defective measles viruses: infection control by the inflammatory and interferon responses of rhesus monkeys. J Virol **2008**; 82:5359–67.
142. Takeda M, Ohno S, Tahara M, et al. Measles viruses possessing the polymerase protein genes of the Edmonston vaccine strain exhibit attenuated gene expression and growth in cultured cells and SLAM knock-in mice. J Virol **2008**; 82:11979–84.
143. Haga T, Murayama N, Shimizu Y, et al. Analysis of antibody response by temperature-sensitive measles vaccine strain in the cotton rat model. Comp Immunol Microbiol Infect Dis **2009**; 32:395–406.
144. Tahara M, Takeda M, Yanagi Y. Altered interaction of the matrix protein with the cytoplasmic tail of hemagglutinin modulates measles virus growth by affecting virus assembly and cell-cell fusion. J Virol **2007**; 81:6827–36.
145. Tahara M, Takeda M, Yanagi Y. Contributions of matrix and large protein genes of the measles virus edmonston strain to growth in cultured cells as revealed by recombinant viruses. J Virol **2005**; 79:15218–25.
146. Dong JB, Saito A, Mine Y, et al. Adaptation of wild-type measles virus to cotton rat lung cells: E89K mutation in matrix protein contributes to its fitness. Virus Genes **2009**; 39:330–4.
147. Johnston IC, ter Meulen V , Schneider-Schaulies J, Schneider-Schaulies S. A recombinant measles vaccine virus expressing wild-type glycoproteins: consequences for viral spread and cell tropism. J Virol **1999**; 73:6903–15.
148. Plemper RK, Compans RW. Mutations in the putative HR-C region of the measles virus F2 glycoprotein modulate syncytium formation. J Virol **2003**; 77:4181–90.
149. Plemper RK, Lakdawala AS, Gernert KM, Snyder JP, Compans RW. Structural features of paramyxovirus F protein required for fusion initiation. Biochemistry **2003**; 42:6645–55.
150. Leonard VH, Hodge G, Reyes-Del Valle J, McChesney MB, Cattaneo R. Measles virus selectively blind to signaling lymphocytic activation molecule (SLAM; CD150) is attenuated and induces strong adaptive immune responses in rhesus monkeys. J Virol **2010**; 84:3413–20.
151. Santiago C, Celma ML, Stehle T, Casasnovas JM. Structure of the measles virus hemagglutinin bound to the CD46 receptor. Nat Struct Mol Biol **2010**; 17:124–9.
152. Bartz R, Brinckmann U, Dunster LM, Rima B, Ter Meulen V, Schneider-Schaulies J. Mapping amino acids of the measles virus hemagglutinin responsible for receptor (CD46) downregulation. Virology **1996**; 224:334–7.
153. Hsu EC, Sarangi F, Iorio C, et al. A single amino acid change in the hemagglutinin protein of measles virus determines its ability to bind CD46 and reveals another receptor on marmoset B cells. J Virol **1998**; 72:2905–16.
154. Lecouturier V, Fayolle J, Caballero M, et al. Identification of two amino acids in the hemagglutinin glycoprotein of measles virus (MV) that govern hemadsorption, HeLa cell fusion, and CD46 downregulation: phenotypic markers that differentiate vaccine and wild-type MV strains. J Virol **1996**; 70:4200–4.
155. Masse N, Ainouze M, Neel B, Wild TF, Buckland R, Langedijk JP. Measles virus (MV) hemagglutinin: evidence that attachment sites for MV receptors SLAM and CD46 overlap on the globular head. J Virol **2004**; 78:9051–63.
156. Masse N, Barrett T, Muller CP, Wild TF, Buckland R. Identification of a second major site for CD46 binding in the hemagglutinin protein from a laboratory strain of measles virus (MV): potential consequences for wild-type MV infection. J Virol **2002**; 76:13034–8.
157. Patterson JB, Scheiflinger F, Manchester M, Yilma T, Oldstone MB. Structural and functional studies of the measles virus hemagglutinin: identification of a novel site required for CD46 interaction. Virology **1999**; 256:142–51.
158. Vongpunsawad S, Oezgun N, Braun W, Cattaneo R. Selectively receptor-blind measles viruses: identification of residues necessary for SLAM- or CD46-induced fusion and their localization on a new hemagglutinin structural model. J Virol **2004**; 78:302–13.
159. Nielsen L, Blixenkrone-Moller M, Thylstrup M, Hansen NJ, Bolt G. Adaptation of wild-type measles virus to CD46 receptor usage. Arch Virol **2001**; 146:197–208.
160. Shibahara K, Hotta H, Katayama Y, Homma M. Increased binding activity of measles virus to monkey red blood cells after long-term passage in Vero cell cultures. J Gen Virol **1994**; 75:3511–6.
161. Tanaka K, Xie M, Yanagi Y. The hemagglutinin of recent measles virus isolates induces cell fusion in a marmoset cell line, but not in other CD46-positive human and monkey cell lines, when expressed together with the F protein. Arch Virol **1998**; 143:213–25.
162. Xie M, Tanaka K, Ono N, Minagawa H, Yanagi Y. Amino acid substitutions at position 481 differently affect the ability of the measles virus hemagglutinin to induce cell fusion in monkey and marmoset cells co-expressing the fusion protein. Arch Virol **1999**; 144:1689–99.
163. Seki F, Takeda M, Minagawa H, Yanagi Y. Recombinant wild-type measles virus containing a single N481Y substitution in its haemagglutinin cannot use receptor CD46 as efficiently as that having the haemagglutinin of the Edmonston laboratory strain. J Gen Virol **2006**; 87:1643–8.
164. Tahara M, Takeda M, Seki F, Hashiguchi T, Yanagi Y. Multiple amino acid substitutions in hemagglutinin are necessary for wild-type measles virus to acquire the ability to use receptor CD46 efficiently. J Virol **2007**; 81:2564–72.
165. Hummel KB, Bellini WJ. Localization of monoclonal antibody epitopes and functional domains in the hemagglutinin protein of measles virus. J Virol **1995**; 69:1913–6.
166. Hummel KB, Vanchiere JA, Bellini WJ. Restriction of fusion protein mRNA as a mechanism of measles virus persistence. Virology **1994**; 202:665–72.
167. Li L, Qi Y. A novel amino acid position in hemagglutinin glycoprotein of measles virus is responsible for hemadsorption and CD46 binding. Arch Virol **2002**; 147:775–86.
168. Rima BK, Earle JA, Baczko K, et al. Sequence divergence of measles virus haemagglutinin during natural evolution and adaptation to cell culture. J Gen Virol **1997**; 78( Pt 1);97–106.
169. Rota JS, Hummel KB, Rota PA, Bellini WJ. Genetic variability of the glycoprotein genes of current wild-type measles isolates. Virology **1992**; 188:135–42.
170. Woelk CH, Jin L, Holmes EC, Brown DW. Immune and artificial selection in the haemagglutinin (H) glycoprotein of measles virus. J Gen Virol **2001**; 82:2463–74.
171. Schnorr JJ, Dunster LM, Nanan R, Schneider-Schaulies J, Schneider-Schaulies S, ter Meulen V. Measles virus-induced down-regulation of CD46 is associated with enhanced sensitivity to complement-mediated lysis of infected cells. Eur J Immunol **1995**; 25:976–84.
172. Alkhatib G, Briedis DJ. The predicted primary structure of the measles virus hemagglutinin. Virology **1986**; 150:479–90.
173. Sakata H, Kobune F, Sato TA, Tanabayashi K, Yamada A, Sugiura A. Variation in field isolates of measles virus during an 8-year period in Japan. Microbiol Immunol **1993**; 37:233–7.
174. Hashiguchi T, Kajikawa M, Maita N, et al. Crystal structure of measles virus hemagglutinin provides insight into effective vaccines. Proc Natl Acad Sci U S A **2007**; 104:19535–40.
175. Bankamp B, Bellini WJ, Rota PA. Comparison of L proteins of vaccine and wild-type measles viruses. J Gen Virol **1999**; 80:1617–25.
176. Bankamp B, Kearney SP, Liu X, Bellini WJ, Rota PA. Activity of polymerase proteins of vaccine and wild-type measles virus strains in a minigenome replication assay. J Virol **2002**; 76:7073–81.
177. Rima BK, Duprex WP. The measles virus replication cycle. Curr Top Microbiol Immunol **2009**; 329:77–102.
178. Liu X, Bankamp B, Xu W, Bellini WJ, Rota PA. The genomic termini of wild-type and vaccine strains of measles virus. Virus Res **2006**; 122:78–84.
179. Kozak M. Point mutations define a sequence flanking the AUG initiator codon that modulates translation by eukaryotic ribosomes. Cell **1986**; 44:283–92.

180. Forcic D, Gulija TK, Jug R, Mazuran R, Baricevic M. Determination of the coding and non-coding nucleotide sequences of genuine Edmonston-Zagreb master seed and current working seed lot. Vaccine **2005**; 23:1072–8.
181. Bellocq C, Mottet G, Roux L. Wide occurrence of measles virus subgenomic RNAs in attenuated live-virus vaccines. Biologicals **1990**; 18:337–43.
182. Calain P, Roux L. Generation of measles virus defective interfering particles and their presence in a preparation of attenuated live-virus vaccine. J Virol **1988**; 62:2859–66.
183. Lazzarini RA, Keene JD, Schubert M. The origins of defective interfering particles of the negative-strand RNA viruses. Cell **1981**; 26:145–54.
184. Whistler T, Bellini WJ, Rota PA. Generation of defective interfering particles by two vaccine strains of measles virus. Virology **1996**; 220:480–4.
185. Shingai M, Ebihara T, Begum NA, et al. Differential type I IFN-inducing abilities of wild-type versus vaccine strains of measles virus. J Immunol **2007**; 179:6123–33.
186. Banerjee K, Shaikh N, Phadke M, Bedekar SS, Rauta SK, Mehta JM. Comparative efficacy of three measles vaccines in Indian children. Indian J Public Health **1998**; 42:113–9.
187. Wu T. The history and current status on measles control in China. Chin J Epidemiol **2004**; 21:143–146.
188. Finsterbusch T, Wolbert A, Deitemeier I, et al. Measles viruses of genotype H1 evade recognition by vaccine-induced neutralizing antibodies targeting the linear haemagglutinin noose epitope. J Gen Virol **2009**; 90:2739–45.
189. Tamin A, Rota PA, Wang ZD, Heath JL, Anderson LJ, Bellini WJ. Antigenic analysis of current wild type and vaccine strains of measles virus. J Infect Dis **1994**; 170:795–801.
190. Klingele M, Hartter HK, Adu F, Ammerlaan W, Ikusika W, Muller CP. Resistance of recent measles virus wild-type isolates to antibody-mediated neutralization by vaccinees with antibody. J Med Virol **2000**; 62:91–8.
191. Centers for Disease Control and Prevention. Elimination of measles–South Korea, 2001–2006. MMWR Morb Mortal Wkly Rep **2007**; 56:304–7.
192. Centers for Disease Control and Prevention. Progress toward the 2012 measles elimination goal–Western Pacific Region, 1990–2008. MMWR Morb Mortal Wkly Rep **2009**; 58:669–73.
193. de Quadros CA, Andrus JK, Danovaro-Holliday MC, Castillo-Solorzano C. Feasibility of global measles eradication after interruption of transmission in the Americas. Expert Rev Vaccines **2008**; 7:355–62.
194. Agocs MM, Markowitz LE, Straub I, Domok I. The 1988–1989 measles epidemic in Hungary: assessment of vaccine failure. Int J Epidemiol **1992**; 21:1007–13.
195. Cutts FT, Markowitz LE. Successes and failures in measles control. J Infect Dis **1994**; 170(Suppl 1):S32–41.
196. Hayden GF. Measles vaccine failure: a survey of causes and means of prevention. Clin Pediatr (Phila) **1979**; 18:155–6161-153, 167.
197. Youwang Y, Ping W, Feng C. Serological and epidemiological effects and influence factors of primary immunization with current live attenuated measles vaccine (Hu191) among infants aged 6–15 months. Vaccine **2001**; 19:1998–2005.
198. Dilraj A, Cutts FT, de Castro JF, et al. Response to different measles vaccine strains given by aerosol and subcutaneous routes to schoolchildren: a randomised trial. Lancet **2000**; 355:798–803.
199. Huang KG, Spence MR, Deforest A, Bradley AT. Measles immunization in HCWs. Infect Control Hosp Epidemiol **1994**; 15:4.
200. Kaplan LJ, Daum RS, Smaron M, McCarthy CA. Severe measles in immunocompromised patients. JAMA **1992**; 267:1237–41.
201. Moss WJ, Cutts F, Griffin DE. Implications of the human immunodeficiency virus epidemic for control and eradication of measles. Clin Infect Dis **1999**; 29:106–12.
202. Permar SR, Griffin DE, Letvin NL. Immune containment and consequences of measles virus infection in healthy and immunocompromised individuals. Clin Vaccine Immunol **2006**; 13:437–43.
203. Helfand RF, Witte D, Fowlkes A, et al. Evaluation of the immune response to a 2-dose measles vaccination schedule administered at 6 and 9 months of age to HIV-infected and HIV-uninfected children in Malawi. J Infect Dis **2008**; 198:1457–65.
204. Nair N, Moss WJ, Scott S, et al. HIV-1 infection in Zambian children impairs the development and avidity maturation of measles virus-specific immunoglobulin G after vaccination and infection. J Infect Dis **2009**; 200:1031–8.
205. Bellini WJ, Rota JS, Lowe LE, et al. Subacute sclerosing panencephalitis: more cases of this fatal disease are prevented by measles immunization than was previously recognized. J Infect Dis **2005**; 192:1686–93.
206. Escoffier C, Gerlier D. Infection of chicken embryonic fibroblasts by measles virus: adaptation at the virus entry level. J Virol **1999**; 73:5220–4.
207. Sharma LB, Ohgimoto S, Kato S, et al. Contribution of matrix, fusion, hemagglutinin, and large protein genes of the CAM-70 measles virus vaccine strain to efficient growth in chicken embryonic fibroblasts. J Virol **2009**; 83:11645–54.
208. Calain P, Roux L. The rule of six, a basic feature for efficient replication of Sendai virus defective interfering RNA. J Virol **1993**; 67:4822–30.

JOURNAL OF VIROLOGY, Nov. 2011, p. 11871–11882 Vol. 85, No. 22
0022-538X/11/$12.00 doi:10.1128/JVI.05067-11


# The SI Strain of Measles Virus Derived from a Patient with Subacute Sclerosing Panencephalitis Possesses Typical Genome Alterations and Unique Amino Acid Changes That Modulate Receptor Specificity and Reduce Membrane Fusion Activity▽‡

Fumio Seki,[1]* Kentaro Yamada,[1]† Yuichiro Nakatsu,[1] Koji Okamura,[2] Yusuke Yanagi,[2] Tetsuo Nakayama,[3] Katsuhiro Komase,[1] and Makoto Takeda[1]

*Department of Virology 3, National Institute of Infectious Diseases, Tokyo,[1] Department of Virology, Faculty of Medicine, Kyushu University, Fukuoka,[2] and Laboratory of Viral Infection I, Kitasato Institute for Life Sciences, Kitasato University, Tokyo,[3] Japan*

Received 10 May 2011/Accepted 31 August 2011

**Subacute sclerosing panencephalitis (SSPE) is a fatal sequela associated with measles and is caused by persistent infection of the brain with measles virus (MV). The SI strain was isolated in 1976 from a patient with SSPE and shows neurovirulence in animals. Genome nucleotide sequence analyses showed that the SI strain genome possesses typical genome alterations for SSPE-derived strains, namely, accumulated amino acid substitutions in the M protein and cytoplasmic tail truncation of the F protein. Through the establishment of an efficient reverse genetics system, a recombinant SI strain expressing a green fluorescent protein (rSI-AcGFP) was generated. The infection of various cell types with rSI-AcGFP was evaluated by fluorescence microscopy. rSI-AcGFP exhibited limited syncytium-forming activity and spread poorly in cells. Analyses using a recombinant MV possessing a chimeric genome between those of the SI strain and a wild-type MV strain indicated that the membrane-associated protein genes (M, F, and H) were responsible for the altered growth phenotype of the SI strain. Functional analyses of viral glycoproteins showed that the F protein of the SI strain exhibited reduced fusion activity because of an E300G substitution and that the H protein of the SI strain used CD46 efficiently but used the original MV receptors on immune and epithelial cells poorly because of L482F, S546G, and F555L substitutions. The data obtained in the present study provide a new platform for analyses of SSPE-derived strains as well as a clear example of an SSPE-derived strain that exhibits altered receptor specificity and limited fusion activity.**

Measles is an acute highly contagious disease characterized by high fever and a maculopapular rash. Acute measles is accompanied by temporary and severe immunosuppression, and pneumonia caused by secondary bacterial infections is a major cause of measles-related death in children. Subacute sclerosing panencephalitis (SSPE) is a fatal sequela associated with measles. It occurs at a mean latency period of 7 to 10 years after the acute measles stage of development (3, 52). SSPE is caused by persistent infection of the central nervous system (CNS) with measles virus (MV), and suffering from acute measles at an early age is a risk factor for developing SSPE (17). A recent analysis indicated that the risk of developing SSPE was 22 cases per 100,000 reported cases of acute measles (3).

The causative agent, MV, is an enveloped virus that belongs to the genus *Morbillivirus* in the family *Paramyxoviridae*. MV possesses a nonsegmented, negative-sense RNA genome that includes six linked tandem genes, N, P/V/C, M, F, H, and L. The genome is encapsidated by the nucleocapsid (N) protein and is associated with a viral RNA-dependent RNA polymerase composed of phosphoproteins (P proteins) and large proteins (L proteins) that form a ribonucleoprotein (RNP) complex (12). Two types of glycoprotein spikes, the hemagglutinin (H) and fusion (F) proteins, are expressed on the viral envelope. The H protein is responsible for binding to cellular receptors on the target host cells. The signaling lymphocyte activation molecule (SLAM) expressed on immune system cells functions as the principal receptor for MV (62, 69). We and another group recently demonstrated that certain epithelial cells that form tight junctions express an unidentified receptor for MV that is designated the epithelial cell receptor (ECR) (25, 50, 59). Binding of the H protein to a receptor triggers F protein-mediated membrane fusion of the virus envelope and the host cell plasma membrane (12). These proteins are also expressed on the cell surface and cause cell-to-cell fusion. The matrix (M) protein plays crucial roles in the process of virus assembly via its interaction with both the RNP and the cytoplasmic tails of the glycoproteins. MV strains derived from patients with SSPE (SSPE strains) generally do not express a functional M protein, becoming defective in producing infectious virus particles, and thus spread via cell-to-cell fusion (10, 14–16, 18). In addition, SSPE strains usually have a deletion or an alteration in the cytoplasmic tail of the F protein (4, 9, 31, 44).

* Corresponding author. Mailing address: Department of Virology 3, National Institute of Infectious Diseases, Gakuen 4-7-1, Musashimurayama 208-0011, Tokyo, Japan. Phone: 81-42-561-0771. Fax: 81-42-562-8941. E-mail: fseki@nih.go.jp.

† Present address: Research Promotion Project, Oita University, Oita, Japan.

‡ Supplemental material for this article may be found at http://jvi.asm.org/.

▽ Published ahead of print on 14 September 2011.

The SI strain was isolated in 1976 from a patient with SSPE by cultivating brain tissue biopsy samples with Vero cells (29). The patient was 8 years of age and had suffered from acute measles at 4 years of age (29). The SI strain was found to show neurovirulence, and all animals (mice, hamsters, and guinea pigs) inoculated intracerebrally with the SI strain showed neurological manifestations at 3 to 6 days after inoculation and eventually died (29). Despite these significant characteristics, molecular analyses of the SI strain have been poorly conducted. In the present study, we identified unique characteristics of the SI strain and identified substitutions responsible for the modulated receptor specificity and reduced membrane fusion activity. The present study also obtained data using a genetic engineering system of the SI strain expressing a fluorescent protein. This system could be a new platform for analyses of the molecular bases and pathogenesis of SSPE.

## MATERIALS AND METHODS

**Cells.** BHK/T7-9 cells constitutively expressing T7 RNA polymerase (20) were maintained in Dulbecco's minimum essential medium (DMEM; Sigma, St. Louis, MO) supplemented with 7% fetal bovine serum (FBS). Vero/hSLAM (36) and CV1/hSLAM (58), which constitutively express human SLAM (hSLAM), were maintained in DMEM supplemented with 7% FBS and 0.5 mg/ml Geneticin (G418; Invitrogen Life Technologies, Carlsbad, CA). CHO cells and A549 cells constitutively expressing human SLAM, CHO/hSLAM (62), and A549/hSLAM (57), respectively, were maintained in RPMI medium (Invitrogen) supplemented with 7% FBS and 0.5 mg/ml G418. Vero cells and IMR-32 cells were maintained in DMEM supplemented with 7% FBS and 10% FBS, respectively. H358 (59) and II-18 (49) cells were maintained in RPMI supplemented with 10% FBS. SH-SY5Y cells were maintained in DMEM/F12 (Invitrogen) supplemented with 10% FBS (49, 59).

**Plasmid constructions.** The first-strand cDNA of the SI strain antigenome was synthesized by reverse transcription of total RNA isolated from Vero/hSLAM cells infected with the SI strain. Eight DNA fragments covering the entire region of the SI strain genome were then generated by PCR. These fragments were cloned into pBluescriptII KS(+) vector (Agilent Technologies, Inc., Santa Clara, CA) in a stepwise manner, generating a plasmid carrying the full-length antigenomic cDNA of the SI strain (detailed procedure provided upon request). A hammerhead ribozyme sequence (HHRz) was added between the T7 promoter sequence and the MV genome cDNA by a combination of PCR procedures using the synthesized DNA (5′-GTGAATTGTAATACGACTCACTATAGGG*GTCTTTG GTCTGATGAGGCCGAAAGGCCGAAACTCCGTAAGGAGTC*ACCAAACA AA-3′; the T7 promoter and HHRz sequences are shown in boldface and italics, respectively, and the MV genome cDNA sequence is underlined). To generate an additional transcriptional unit for a green fluorescent protein (GFP) derived from *Aequorea coerulescens* (AcGFP; Clontech, Palo Alto, CA), a fragment containing the open reading frame (ORF) of AcGFP was amplified by PCR using primer pair 5′-*GGCGCGCC*ATGGTGAGCAAG-3′ and 5′-*GACGTC*TT ACTTGTACAGCTCGT-3′ (sequences corresponding to the AscI and AatII sites are shown in italics; sequences corresponding to the initiation and termination codons are shown in boldface). The fragment was combined with the synthesized cDNA fragments containing the region between the H and L protein open reading frames of the IC-B strain by a combination of PCR procedures. The nucleotide sequences of the synthesized cDNA fragments were 5′-ACTAGTGAAATAGACA TCAGAATTAAGAAAAACGTAGGGTCCAAGTGGTTTCCCGTT*GGCGCG CC*-3′ and 5′-*GACGTC*TGCCAGTGAACCGATCACATGATGTCACCCAGAC ATCAGGCATACCCACTAGT-3′ (sequences corresponding to SpeI sites are shown in boldface, sequences corresponding to AscI and AatII sites are shown in italics, and sequences corresponding to the gene end [GE] of the H gene and gene start [GS] of the L gene are underlined). The fragment containing the transcriptional unit for AcGFP was then inserted into the SpeI site between the H and L genes. The generated construct was named pHHRz-SI-AcGFP. Using a similar procedure, the additional transcriptional unit for AcGFP was also inserted into the p(+)MV323 plasmid, which carries the full-length antigenomic cDNA of the IC-B strain (60). The resulting plasmid was named p(+)MV323-AcGFP. A SalI-AatII fragment containing a region of the M, F, and H genes of p(+)MV323-AcGFP was replaced with a corresponding fragment of pHHRz-SI-AcGFP, and the generated construct was named p(+)MV323/SI-MFH-AcGFP. A SalI-BstEII fragment containing a region of the M gene of the pHHRz-SI-AcGFP was replaced with a corresponding fragment of p(+)MV323, and the generated construct was named pHHRz-SI/ICM-AcGFP. To generate support plasmids for the rescue of recombinant MVs from cloned cDNAs, DNA fragments encoding the N, P, and L proteins of the wild-type (wt) MV strains (IC-B or 9301B) were cloned into the pCITE vector (Novagen, Madison, WI), generating pCITE-IC-N, pCITE-IC-PΔC, and pCITEko-9301B-L, respectively. DNA fragments encoding the M proteins of the IC-B and SI strains fused with a red fluorescent protein, mCherry (Clontech), at the carboxyl-terminal end were generated by a combination of PCR procedures and inserted into a mammalian expression vector, pCA7 (32, 57). The resulting plasmids were named pCA7-FR-IC-M-mCherry and pCA7-FR-SI-mCherry, respectively. DNA fragments encoding the F proteins of the IC-B and SI strains were also amplified by PCR and cloned into pCAGGS (32), generating pCAGGS-IC-F and pCAGGS-SI-F, respectively. Similarly, DNA fragments encoding the H proteins of the IC-B and SI strains were amplified and cloned into pCAGGS, generating pCAGGS-IC-H and pCAGGS-SI-H, respectively. By replacing the SalI-XhoI, EcoRI-SalI, KpnI-XhoI, and SalI-KpnI regions of pCAGGS-IC-F with the corresponding region of pCAGGS-SI-F, four plasmids encoding chimeric F proteins between the IC-B and SI strains, designated pCAGGS-IC/SI-F-1, -F-2, -F-3, and -F-4, respectively, were generated. An amino acid substitution, G300E, was introduced into pCAGGS-SI-F, and five other amino acid substitutions, N390M, L482F, S546G, F555L, and I564L, were introduced independently into pCAGGS-IC-H by site-directed mutagenesis using complementary primer pairs.

**Antibodies.** A mouse monoclonal antibody (MAb) against CD46 (M75) was kindly provided by T. Seya (46). Mouse MAbs against the proteins encoded by MV H (B5), F (C527), and M (A23, A24, A27, A154, A157, A177, B46, A39, A41, A42, A51, and A133) were kindly provided by T. A. Sato (42).

**Viruses.** BHK/T7-9 cells were transfected with full-length genome plasmids carrying the antigenomes of MV and three support plasmids, pCITE-IC-N, pCITE-IC-PΔC, and pCITEko-9301B-L, by the use of Lipofectamine LTX Plus reagent (Invitrogen). After 2 days, the transfected cells were cocultured with Vero/hSLAM cells. IC323-AcGFP, SI-AcGFP, IC/SI-MFH-AcGFP, and SI/ICM-AcGFP were generated from p(+)MV323-AcGFP, pHHRz-SI-AcGFP, p(+)MV323/SI-MFH-AcGFP, and pHHRz-SI/ICM-AcGFP, respectively. The generated MVs were propagated in Vero/hSLAM cells. Infectious virus-like particles of SI-AcGFP and IC/SI-MFH-AcGFP were prepared by incubating the cells with 5 μg/ml cytochalasin D (Sigma) at 35°C for 30 min, as described previously (19). The infectious virus-like particles were concentrated using PEG-it precipitation solution (System Biosciences Inc., Mountain View, CA). The cell infectious units (CIUs) of the recombinant MVs expressing a fluorescent protein were determined using Vero/hSLAM cells, as described previously (51). To analyze the cytopathic effects (CPEs), monolayers of cells in 6-well cluster plates were infected with 500 CIUs of MV and the cells were observed daily using an Axio Observer.D1 microscope (Carl Zeiss, Jena, Germany).

**Virus growth.** Monolayers of Vero/hSLAM cells in 24-well plates were infected with recombinant MVs at a multiplicity of infection (MOI) of 0.01 per cell. At various time intervals, cell-free virus was obtained from the culture supernatants, and cell-associated virus was recovered from infected cells in 0.5 ml of DMEM-supplemented 7% FBS by freezing and thawing.

**Virus titration.** Monolayers of Vero/hSLAM cells in 6-well cluster plates were infected with serially diluted virus samples, incubated for 1 h at 37°C, and overlaid with DMEM containing 7% FBS and 1% agarose. PFU numbers were determined by counting the number of plaques.

**Phylogenic tree analysis and Ka/$K_s$ calculation.** Nucleotide and amino acid sequence alignments and a phylogenic distance analysis were performed with the ClustalW program (63) at the genomeNet website maintained by the Kyoto University Bioinformatics Center. A phylogenic tree constructed using SI, IC-B, 9301B, WA.USA/17.98, and reference strains (66) was drawn using FigTree software. Ka/$K_s$ calculations were performed using KaKs Calculator version 2.0 software (64). Briefly, using the two nucleotide sequences of each protein-coding region, the nonsynonymous and synonymous substitution rates (Ka and $K_s$, respectively) were calculated by counting the numbers of nonsynonymous and synonymous sites (NA and NS, respectively) and the numbers of nonsynonymous and synonymous substitutions (MA and MS, respectively). MA/NA and MS/NS represent the Ka and $K_s$ substitution rates, respectively.

**Immunofluorescence staining.** Monolayers of Vero/hSLAM cells were seeded in 24-well plates or on coverslips in six-well cluster plates. Some monolayers were transfected with expression plasmids encoding M protein tagged with mCherry or not tagged. Other monolayers were infected with recombinant MVs and incubated with 50 μg/ml of a fusion-blocking peptide, Z-D-Phe-Phe-Gly (Peptide Institute Inc., Osaka, Japan), as described previously (41). At 24 h posttransfection or at 2 or 5 days postinoculation (p.i.) (using IC323-AcGFP or SI-AcGFP,

respectively), the cells were fixed and permeabilized with phosphate-buffered saline containing 2.5% formaldehyde and 0.5% Triton X-100. The cells were then stained with a mouse MAb against the M protein for 1 h at room temperature, followed by incubation with an Alexa Fluor 488- or 594-conjugated secondary antibody (Molecular Probes, Eugene, OR) for 1 h at room temperature. The nuclei of the infected cells were stained with 4′,6′-diamidino-2-phenylindole (DAPI; Nacalai Tesque, Kyoto, Japan) at 0.2 μg/ml. The cells were observed using a FluoView FV1000 confocal microscope (Olympus, Tokyo, Japan).

**Cell-to-cell fusion assay.** CHO/hSLAM, CV1/hSLAM, Vero, H358, or II-18 cells were seeded in 24-well plates, transfected with the H protein-expressing plasmid (0.5 μg) together with the F protein-expressing plasmid (0.5 μg), and incubated in the presence or absence of an anti-CD46 antibody (M75). At 1, 2, or 3 days posttransfection, the cells were fixed with methanol and stained with Giemsa solution (Sigma). The stained cells were observed under an Axio Observer.D1 microscope. To quantify cell-to-cell fusion, monolayers of cells were transfected with H protein-expressing plasmid (0.3 μg) and F protein-expressing plasmid (0.3 μg) together with a red fluorescent protein (mCherry)-expressing plasmid (0.3 μg). At 48 h posttransfection, areas expressing mCherry autofluorescence were measured using an Axio Observer.D1 microscope and ImageJ software (http://rsbweb.nih.gov/ij/index.html). Statistical analyses were performed using Microsoft Excel version 14.1.2 software.

**Flow cytometry.** CHO/hSLAM cells were transfected with the H or F protein-expressing plasmid (0.5 μg). At 24 h posttransfection, the cells were incubated with mouse MAbs B5 and C527 specific for the H and F proteins, respectively, followed by incubation with an Alexa Fluor 488-conjugated goat anti-mouse secondary antibody (Molecular Probes). The cells were analyzed using a FACSCalibur flow cytometer (Becton Dickinson, Franklin Lakes, NJ).

**Minigenome assay.** BHK/T7-9 cells were transfected with 0.2 μg of p18MGFLuc01 minigenome plasmid (23) together with 0.2 μg of pCITE-IC-N and various amounts of pCITE-IC-PΔC and pCITEko-9301B-L. At 48 h posttransfection, the enzymatic activity of firefly luciferase was measured using a Dual Glo luciferase assay system (Promega, Madison, WI) and a Mithras LB 940 luminometer (Berthold Technologies, Bad Wildbad, Germany).

**Nucleotide sequence accession number.** The nucleotide sequence of the SI strain is available under GenBank accession number JF791787.

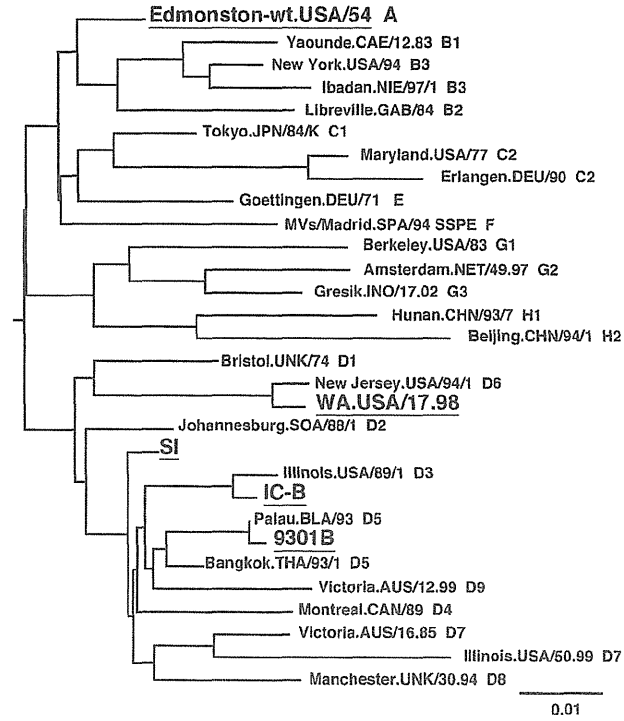


FIG. 1. Phylogenic tree drawn on the basis of the 450-nucleotide sequence that encodes the carboxyl-terminal 150 amino acids of the N protein. The names of the strains used for sequence comparisons in this study (Edmonston-wt, SI, IC-B, 9301B, and WA.USA/17.98) are underlined.

## RESULTS

**Characterization of the genome of the SI strain.** We determined the entire genome nucleotide sequence of the SI strain. A phylogenic tree drawn on the basis of the 450-nucleotide sequence that encodes the carboxyl-terminal 150 amino acids of the N protein showed that the SI strain was classified into clade D but did not belong to a specific genotype (Fig. 1). Genotype analyses performed using a program at a website for measles nucleotide surveillance (MeaNS) (http://www.hpa-bioinformatics.org.uk/Measles/Public/Web_Front/main.php) confirmed the data for the phylogenic tree analysis (see Table S1 in the supplemental material). The entire genome nucleotide sequence of the SI strain was compared with those of three other strains in clade D, strain IC-B (genotype D3; GenBank accession number NC_001498), strain 9301B (genotype D5; GenBank accession number AB012948), and strain WA.USA/17.98 (genotype D6; GenBank accession number DQ227321) (2, 54, 61). The nucleotide sequences of the regulatory regions (i.e., the gene start, gene end, and integenic sequences) (38) were highly conserved in the SI strain genome. As indicated in previous reports (9, 11, 68), highly biased uracil-to-cystine substitutions were observed in the M gene (see Table S2 in the supplemental material). As also observed for other SSPE strains, nonsynonymous substitutions were accumulated in the M protein reading frame of the SI strain (see Fig. S1 in the supplemental material). The data for the comparison between the SI and IC-B strains are shown in the present paper, but similar results were obtained in the comparisons between the SI and other clade D MV strains. The Ka/$K_s$ ratios were analyzed to reveal differences between the SI and clade D MV strains (IC/SI, 9301/SI, and WA98/SI) and between the Edmonston wild-type (wt) strain (genotype A; GenBank accession number AF266288) and clade D MV strains (IC/Edwt, 9301/Edwt, and WA98/Edwt) (37) (the phylogenic tree in Fig. 1 shows the relationships among the SI, IC-B, 9301B, WA.USA/17.98, and Edmonston wt strains). The data of comparisons between the Edmonston wt and clade D MV strains mostly reflect the selection pressure that operated during the natural evolution of wt MVs, while the data showing comparisons between the SI and clade D MV strains reflect the selection pressure that operated during persistent infection in the brain in addition to the natural evolution of MV. Previously, a similar study was performed by Woelk et al. (67). For the M protein reading frame, the Ka/$K_s$ ratios in the comparisons between the Edmonston wt and clade D MV strains were ~0.03, whereas the ratios in the comparisons between the SI and clade D MV strains were 11 to 12 times greater than those observed in comparisons between the Edmonston wt and clade D MV strains (Table 1), confirming that a dynamic selection or a reduced stabilizing selection pressure operated for the M protein of the SI strain, as observed for other SSPE strains (67). Similarly, although the amino acid sequence of the F protein was highly conserved during the natural evolution of MV (Ka/$K_s$ = 0.0000 ~ 0.0359), this was not the case during persistent infection in the brain (Ka/$K_s$ = 0.1825 ~ 0.2504) (Table 1). Compared with those of IC-B, 12 amino acid changes were found in the F protein of the SI strain, including

TABLE 1. $K_s$, Ka, and Ka/$K_s$ values from comparisons of Edmonston wild-type, IC-B, 9301B, WA.USA/17.98, and SI strains[a]

| Protein reading frame | Gene region(s) | Nucleotides[b] | $K_s$ | | Ka | | Ka/$K_s$ | |
|---|---|---|---|---|---|---|---|---|
| | | | IC(D3)/Edwt, 9301(D5)/Edwt, WA98(D6)/Edwt | IC(D3)/SI, 9301(D5)/SI, WA98(D6)/SI | IC(D3)/Edwt, 9301(D5)/Edwt, WA98(D6)/Edwt | IC(D3)/SI, 9301(D5)/SI, WA98(D6)/SI | IC(D3)/Edwt, 9301(D5)/Edwt, WA98(D6)/Edwt | IC(D3)/SI, 9301(D5)/SI, WA98(D6)/SI |
| N | | 1–1578 | 0.0790, 0.0960, 0.1033 | 0.0512, 0.0703, 0.1218 | 0.0117, 0.0113, 0.0092 | 0.0046, 0.0050, 0.0075 | 0.1486, 0.1178, 0.0892 | 0.0898, 0.0712, 0.0618 |
| P | P | 1–1524 | 0.0416, 0.0443, 0.0330 | 0.0246, 0.0273, 0.0330 | 0.0114, 0.0176, 0.0132 | 0.0079, 0.0141, 0.0096 | 0.2740, 0.3981, 0.3982 | 0.3195, 0.5150, 0.2918 |
| | P/C | 22–582 | 0.0222, 0.0223, 0.0297 | 0.0073, 0.0074, 0.0147 | 0.0191, 0.0239, 0.0215 | 0.0024, 0.0071, 0.0047 | 0.8596, 1.0739, 0.7241 | 0.3217, 0.9645, 0.3212 |
| | P/V | 691–903 | 0.0178, 0.0177, 0 | 0.0177, 0.0176, 0 | 0, 0.0064, 0.0129 | 0.0195, 0.0262, 0.0327 | 0, 0.3643, NA[c] | 1.0991, 1.4842, NA |
| | P′ | 1–21 + 583–690 + 904–1524 | 0.0648, 0.0704, 0.0465 | 0.0405, 0.0461, 0.0585 | 0.0088, 0.0160, 0.0071 | 0.0088, 0.0160, 0.0071 | 0.1361, 0.2272, 0.1516 | 0.2179, 0.3472, 0.1206 |
| C | | 1–561 | 0.0464, 0.0705, 0.0543 | 0.0075, 0.0305, 0.0151 | 0.0119, 0.0095, 0.0143 | 0.0024, 0, 0.0047 | 0.2561, 0.1345, 0.2629 | 0.3132, 0, 0.3127 |
| V | V trans[d] | 690–902 | 0, 0.0217, 0.0439 | 0.0434, 0.0667, 0.0902 | 0.0063, 0, 0 | 0.0063, 0, 0 | NA, 0, 0 | 0.1449, 0, 0 |
| M | | 1–1008 | 0.0842, 0.0936, 0.0892 | 0.2135, 0.2134, 0.2141 | 0.0026, 0.0026, 0.0026 | 0.0758, 0.0758, 0.0772 | 0.0310, 0.0279, 0.0293 | 0.3551, 0.3552, 0.3606 |
| F | | 1–1653 | 0.0566, 0.0627, 0.0675 | 0.0355, 0.0459, 0.0621 | 0, 0.0024, 0.0024 | 0.0089, 0.0113, 0.0113 | 0, 0.0359, 0.0357 | 0.2504, 0.2470, 0.1825 |
| H | | 1–1854 | 0.0902, 0.0877, 0.0724 | 0.0675, 0.0651, 0.0907 | 0.0114, 0.0100, 0.0092 | 0.0085, 0.0071, 0.0135 | 0.1263, 0.1135, 0.1276 | 0.1262, 0.1089, 0.1490 |
| L | | 1–6549 | 0.0801, 0.0927, 0.0822 | 0.0601, 0.0687, 0.0781 | 0.0047, 0.0051, 0.0049 | 0.0050, 0.0054, 0.0058 | 0.0584, 0.0548, 0.0594 | 0.0828, 0.0782, 0.0739 |

[a] Edwt, Edmonston wild type; IC(D3), IC-B; 9301(D5), 9301B; WA98(D6), WA.USA/17.98.
[b] The first nucleotide of the initiation codon for each open reading frame is taken as 1.
[c] NA, not applicable.
[d] V trans is the C-terminal region unique to the V protein.

a nonsense mutation at amino acid position 532 (Table 2). These changes in the F protein are typical of SSPE strains (4, 9, 31, 44). For the N, H, and L protein reading frames, in contrast, the Ka/$K_s$ ratios revealed by the comparisons between the SI and clade D MV strains were similar to those observed between the Edmonston wt and clade D MV strains (Table 1). These data indicated that similar levels of stabilizing selection pressure operated for the N, H, and L protein reading frames of the SI strain during the persistent infection in the brain. For the P gene, it was not simple to assess the data for the Ka and $K_s$ values, since the gene contains overlapping reading frames. Nonetheless, it was evident that both the C and V nonstructural proteins were highly conserved during the persistent infection in the brain. For the C protein-reading frame, the Ka values for the IC/SI and WA93/SI comparisons were as much as 3 to 5 times lower than those for the IC/Edwt and WA93/SI comparisons (Table 1). Indeed, no amino acid substitution was found in the C protein of the SI strain compared with that of the 9301B strain. Similarly, no amino acid substitution was found in the V protein-unique region of the SI strain compared with that of the WA.USA/17.98. strain. The V protein-unique region of the 9301B strain also had the same amino acid sequence as those of the SI and WA.USA/17/98 strains except that the 9301B V protein possessed an additional single amino acid at the carboxyl-terminal end, because it terminated one codon later (since this additional codon was not included in calculation, the Ka of 9301/SI comparison was zero [Table 1]). These data suggested that both the C and V proteins played important roles in the survival of the SI strain in the brain.

**Generation of a recombinant SI strain expressing a fluorescent protein by establishment of an efficient MV rescue system.** The SI strain did not produce cell-free infectious particles and spread poorly in cell cultures (data not shown). In addition, a CPE was barely detectable in some cultured cells, although the SI strain replicated in them (data not shown). Many studies have shown that the use of recombinant viruses genetically engineered to express a fluorescent protein is greatly advantageous for monitoring virus infections, especially when the virus infection shows a small or weak CPE. Therefore, we decided to generate a recombinant SI strain expressing a fluorescent protein. A full-length genome cDNA of the SI strain possessing an additional transcriptional unit encoding AcGFP between the H and L genes was generated and inserted into the pBluescript vector downstream of the T7 promoter (Fig. 2). The T7 promoter was followed by three guanines that enhance the transcription efficiency (Fig. 2). Since these guanines produce extra guanine residues at the 5′ end of the synthesized MV antig-

TABLE 2. Amino acid substitutions in the F proteins among the IC, SI, and Edmonston strains

| Amino acid no. | Amino acid substitution(s) or category | | |
|---|---|---|---|
| | IC | SI | Ed |
| 78 | R | G | R |
| 165 | R | K | R |
| 167 | A | T | A |
| 187 | I | V | I |
| 242 | I | T | I |
| 246 | L | F | L |
| 247 | E | K | E |
| 268 | G | D | G |
| 300 | E | G | E |
| 487 | M | I | M |
| 532 | R | Stop | R |
| 533–550 | 18 aa[a] | Deletion | 18 aa |

[a] aa, amino acids.

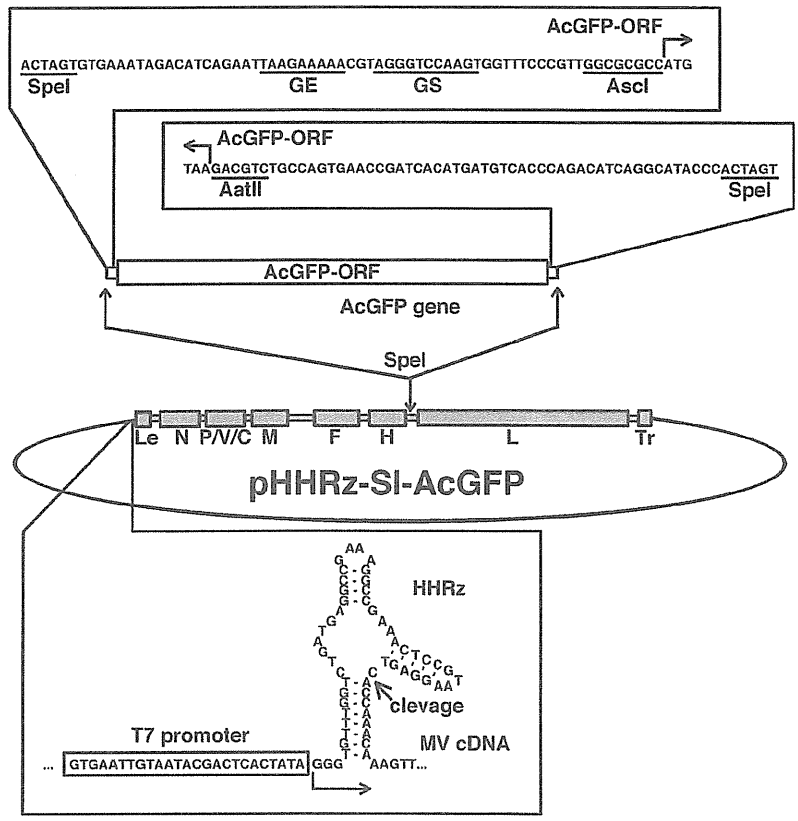


FIG. 2. Diagram of the genome plasmid with insertion of an additional transcriptional unit and the HHRz sequence. Transcriptional regulatory regions (gene end [GE], intergenic, and gene start [GS] sequences) and the coding sequence for AcGFP (AcGFP-ORF) were inserted at the junction between the H and L genes by the use of appropriate restriction enzyme recognition sites (SpeI, AscI, and AatII). The recombinant genome also possesses an HHRz upstream the authentic virus genome.

enome, a precise 5′ end for the MV antigenome was created by inserting HHRz between the three guanines and the first viral nucleotide (Fig. 2). The resulting full-length genome plasmid was designated pHHRz-SI-AcGFP. BHK/T7-9 cells, which represent a baby hamster kidney (BHK) cell-derived clone constitutively expressing T7 RNA polymerase (20) (kindly provided by M. Sugiyama and N. Ito), has been shown to be highly potent for initiating the replication cycles of other negative-strand RNA viruses from cloned cDNAs (20, 48). By the use of previously reported methods of studies employing BHK/T7-9 cells (48), the cDNAs of the N, P, and L genes of MV were inserted into the pCITE vector; the resulting plasmids were termed pCITE-IC-N, pCITE-IC-PΔC, and pCITEko-9301B-L, respectively. These plasmids were designed to create an internal ribosome entry site at the 5′ terminus of the N, P, and L mRNAs. Since the ratios of the plasmids expressing the N, P, and L proteins were previously reported to be critical for the initiation of infectious cycles of paramyxoviruses from cloned cDNAs (13, 21, 26), the optimal ratio for these plasmids was determined using a minireplicon assay for MV (23). The analyses indicated that 0.20, 0.15, and 0.40 μg of pCITE-IC-N, pCITE-IC-PΔC, and pCITEko-9301B-L, respectively, were optimal for the expression of the MV minireplicon gene (luciferase) in BHK/T7-9 cells cultured in a 24-well cluster plate (see Table S3 in the supplemental material). When BHK/T7-9 cells cultured in a 6-well cluster plate were transfected with 5.0 μg of pHHRz-SI-AcGFP together with three support plasmids (0.80, 0.60, and 1.60 μg of pCITE-IC-N, pCITE-IC-PΔC, and pCITEko-9301B-L, respectively), infectious cycles of rSI-AcGFP were efficiently initiated from pHHRz-SI-AcGFP. Subsequently, the recombinant SI strain expressing AcGFP

TABLE 3. Detection of the M protein by an indirect immunofluorescence assay

| MAb clone no. | Antigenic site | Assay result | | | |
|---|---|---|---|---|---|
| | | IC323-AcGFP | SI-AcGFP | IC-M–mCherry | SI-M–mCherry |
| A23 | II | + | – | + | – |
| A24 | II | + | – | + | – |
| A27 | II | + | – | + | – |
| A154 | II | + | – | + | – |
| A157 | II | + | – | + | – |
| A177 | II | + | – | + | – |
| B46 | II | + | – | + | – |
| A39 | III | + | – | + | – |
| A41 | III | + | – | + | – |
| A42 | III | + | – | + | – |
| A51 | III | + | – | + | – |
| A133 | IV | + | – | + | – |

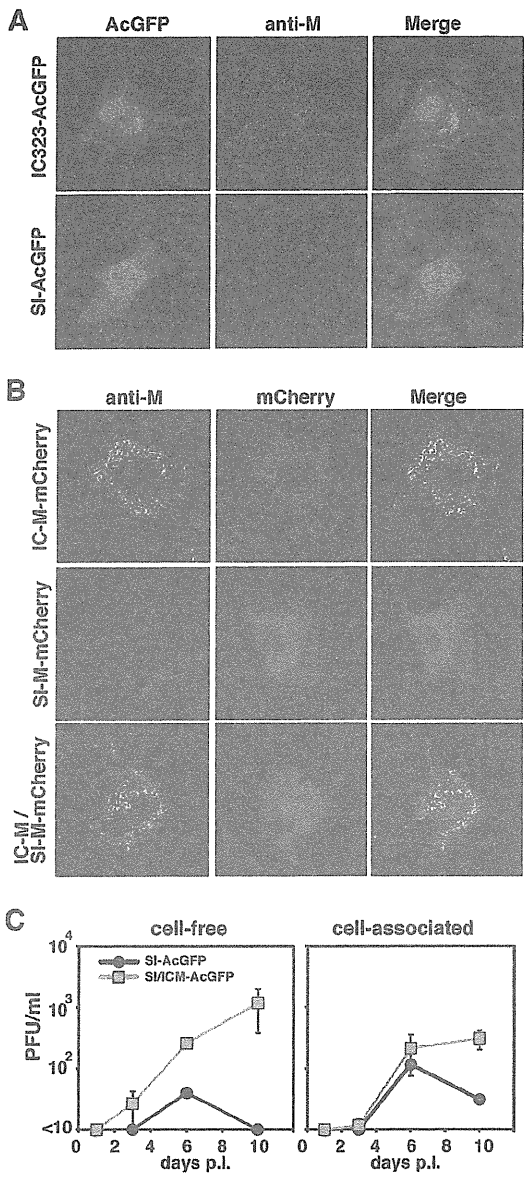


FIG. 3. Distribution of the M protein and effect on viral growth of strain SI possessing the IC-M gene. (A) Distribution of the M protein in cells infected with recombinant MV. Vero/hSLAM cells were infected with IC323-AcGFP or SI-AcGFP. At 2 (IC323-AcGFP) or 5 (SI-AcGFP) days postinfection, the cells were stained with an anti-M protein MAb (A42) and an Alexa Fluor 594-conjugated anti-mouse secondary antibody. The nuclei were stained with DAPI (blue). (B) Distribution of the mCherry-fused M protein. Vero/hSLAM cells were transfected with the M protein-expressing plasmids IC-M-mCherry, SI-M-mCherry, and IC-M plus SI-M-mCherry. At 1 day posttransfection, the cells were stained with an anti-M protein MAb (A42) and an Alexa 488-conjugated anti-mouse secondary antibody. The cells were observed under a confocal microscope. (C) Replication kinetics of recombinant MVs. Vero/hSLAM cells were infected with recombinant MVs at an MOI of 0.01, and infectious titers in culture medium (cell-free) and cells (cell-associated) were determined at 1, 3, 6, and 10 days p.i. Data represent the means ± standard deviations (SD) of results from triplicate samples.

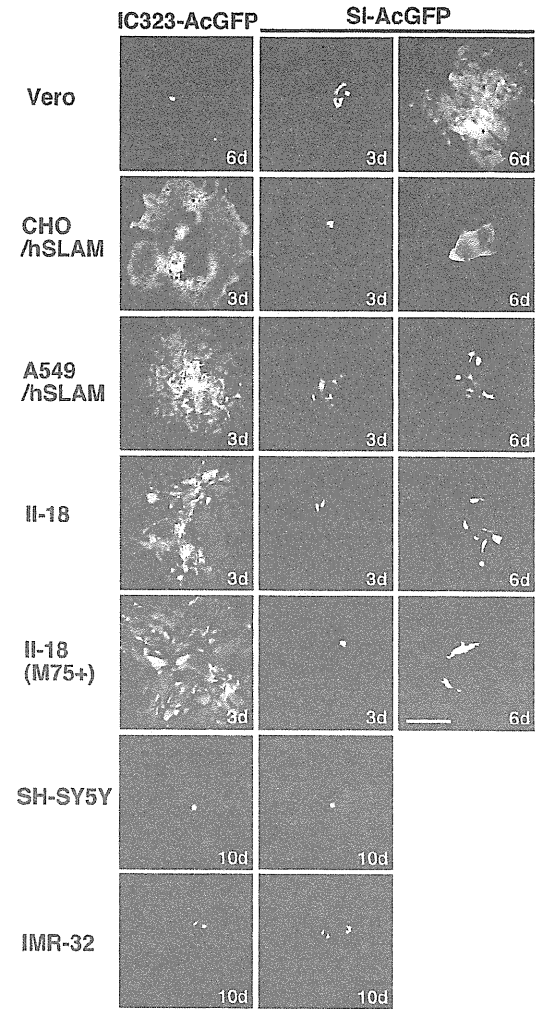


FIG. 4. AcGFP autofluorescence in cells infected with IC323-AcGFP and SI-AcGFP. Vero, CHO/hSLAM, A549/hSLAM, II-18, SH-SY5Y, and IMR-32 cells were infected with IC323-AcGFP or SI-AcGFP. Some II-18 cells were incubated with an anti-CD46 MAb (M75). The cells were observed under a fluorescence microscope at the indicated days (d). Bar, 0.20 mm.

(rSI-AcGFP) was maintained in Vero/hSLAM cells cocultured with BHK/T7-9 cells.

**Properties of the M protein of the SI strain.** Using various MAbs against the M protein (42), an indirect immunofluorescence assay was performed. A total of 12 MAbs that have been shown to recognize antigenic sites II, III, and IV of the M protein were used (42) (Table 3). A recombinant IC323 strain expressing AcGFP (IC323-AcGFP) was generated and used as a control. The IC323 strain is a recombinant MV based on the wt IC-B strain (60). In cells infected with IC323-AcGFP, all the MAbs detected the M protein (Fig. 3A and Table 3). However, in cells infected with the SI or rSI-AcGFP strains, all the MAbs failed to detect the M protein (Fig. 3A and Table 3 and data not shown). These data suggested a lack of M protein expression in cells infected with the SI and rSI-AcGFP strains. Sato et al. (43) also previously showed that M protein expression

TABLE 4. Amino acid substitutions in the H proteins of the IC, SI, and Edmonston strains

| Amino acid no. | Amino acid substitution | | |
|---|---|---|---|
| | IC | SI[a] | Ed[b] |
| 7 | R | Q* | R |
| 71 | H | R* | H |
| 174 | A | A | T |
| 176 | A | A | T |
| 211 | S | S | G |
| 235 | G | E | E |
| 243 | G | G | R |
| 252 | H | H | Y |
| 276 | F | F | L |
| 284 | F | F | L |
| 296 | F | F | L |
| 302 | R | R | G |
| 334 | R | Q | Q |
| 390 | N | M* | I |
| 416 | N | N | D |
| 446 | T | S | S |
| 481 | N | N | Y |
| 482 | L | F* | L |
| 484 | T | T | N |
| 546 | S | G* | S |
| 555 | F | L* | F |
| 564 | I | L* | I |
| 575 | K | Q | Q |
| 600 | V | V | E |

[a] Asterisks indicate amino acids unique to the SI strain.
[b] Edmonston strain; GenBank accession number K01711.

was missing in cells infected with the SI strain. The M proteins of the SI and IC-B strains were expressed in cells by the use of expression plasmids. The carboxyl termini of the M proteins were tagged with mCherry red fluorescent protein. All the MAbs detected the IC-B strain-derived M protein despite the mCherry tag (Table 3). In contrast, none of the MAbs detected the SI strain-derived M protein, although bright mCherry fluorescence was detected in these cells (Fig. 3B and Table 3). These data indicated that the antigenicity of the M protein of the SI strain was totally different from that of the M protein of the IC-B strain and that none of the MAbs recognizing antigenic sites II, III, and IV reacted with the M protein of the SI strain. Therefore, we could not reach a conclusion as to whether the M protein was expressed in cells infected with the SI strain. However, analyses using the expression plasmids demonstrated that, unlike the M protein of the IC-B strain, the M protein of the SI strain was distributed homogeneously in cells (Fig. 3B). The M protein of the IC-B strain was distributed beneath the plasma membrane and formed small dots in the cytoplasm (Fig. 3B). To elucidate the functional difference between the IC-B and SI strains with respect to the M gene, we generated a recombinant MV with a modified SI strain genome in which the M gene was replaced with the M gene of the IC-B strain. The resulting recombinant MV was designated SI/ICM-AcGFP. A growth kinetics analysis showed that, unlike SI-AcGFP, SI/ICM-AcGFP produced cell-free virus well and the cell-free virus titer of SI/ICM-AcGFP was ~1,000 times higher than that of the SI-AcGFP at 10 days p.i. (Fig. 3C). The result demonstrated that SI-M protein was less involved in the budding stage. With these data, we concluded that the SI strain does not express a functional M protein.

**The SI strain exhibits limited syncytium-forming activity.** Various types of cells were infected with SI-AcGFP and IC323-AcGFP. IC323-AcGFP poorly entered Vero cells (SLAM$^-$/CD46$^+$) and did not produce a syncytium (Fig. 4). On the other hand, SI-AcGFP was able to produce syncytia in Vero cells (Fig. 4). Table 4 shows the amino acid substitutions in the H protein. Among them, the S546G substitution is the one that probably contributed to the ability of SI-AcGFP to produce syncytia in Vero cells, because this mutation allows MV to use CD46 as a receptor (69). On the other hand, SI-AcGFP failed to produce syncytia in II-18 cells (ECR$^+$, CD46$^+$), although IC323-AcGFP replicated and produced syncytia in these cells efficiently (Fig. 4). An MAb against CD46 (M75) had a neutral effect on the SI-AcGFP infection of II-18 cells. Similar results were obtained for the infection of SLAM-positive cells (CHO/hSLAM, A549/hSLAM). SI-AcGFP produced syncytia poorly in these cells, whereas IC323-AcGFP produced syncytia very efficiently. These data demonstrate that the SI strain has limited activity in inducing syncytia in SLAM- or ECR-expressing cells, although it has acquired the ability to use CD46 as an alternative receptor. Although three neural cell lines (SK-N-SH, IMR-32, and SH-SY5Y) were infected with SI-AcGFP and IC323-AcGFP, no syncytia were observed in these cells (Fig. 4 and data not shown).

**The membrane-associated protein genes (M, F, and H) determine the growth phenotype of the SI strain.** The amino acid sequences of the RNP component proteins (N, P, and L pro-

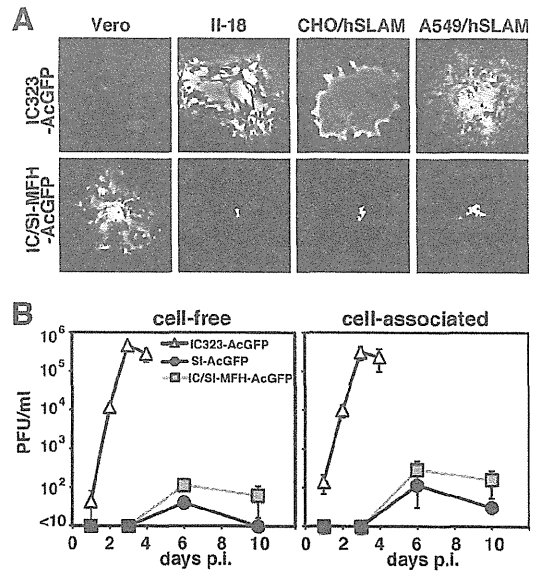


FIG. 5. Effect on viral growth of strain IC possessing the SI-MFH gene in various cell lines. (A) AcGFP fluorescence in cells infected with recombinant MVs. Vero, II-18, CHO/hSLAM, and A549/hSLAM cells were infected with IC323-AcGFP or IC323/SI-MFH-AcGFP. The cells were observed under a fluorescence microscope at 3 (II-18, CHO/hSLAM, and A549/hSLAM) and 6 (Vero) days postinfection. (B) Replication kinetics of recombinant MVs. Vero/hSLAM cells were infected with recombinant MVs at an MOI of 0.01. At various time intervals, infectious titers in culture medium (cell-free) and cells (cell-associated) were determined. Data represent the means ± standard deviations (SD) of the results of experiments performed with triplicate samples.

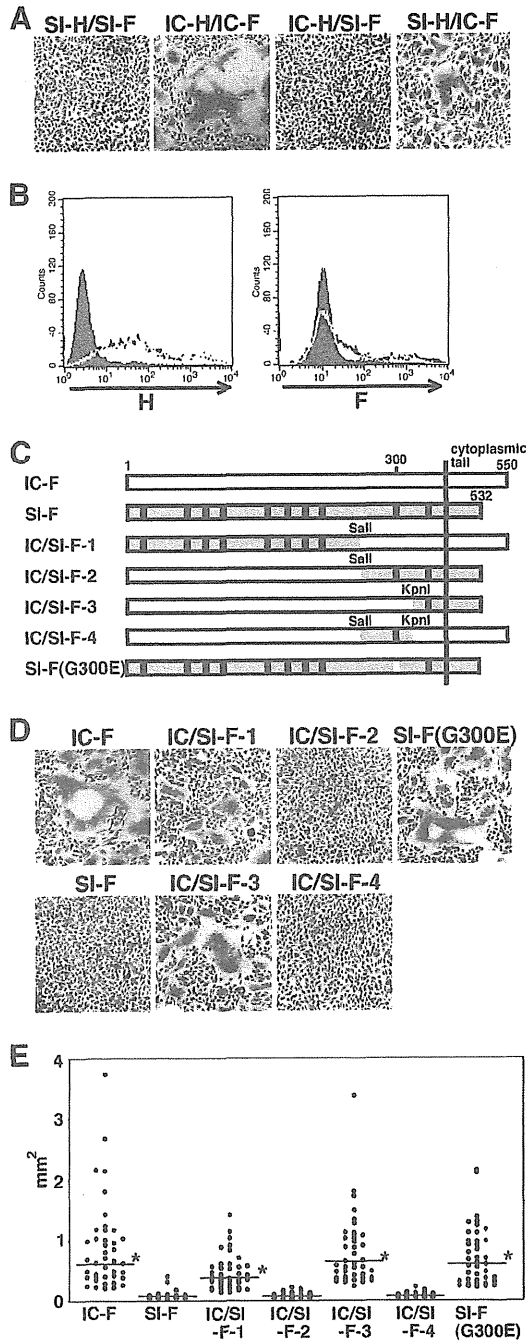


FIG. 6. Syncytium formation in cells expressing H and F proteins and identification of the amino acid residue in the F protein of the SI strain critical for reducing cell-to-cell fusion. (A) Syncytium formation in cells expressing H and F proteins of the IC-B or SI strains. CHO/hSLAM cells were transfected with a plasmid expressing the H protein of the IC-B or SI strain (IC-H or SI-H, respectively) together with a plasmid expressing the F protein of the IC-B or SI strain (IC-F or SI-F, respectively). At 24 h posttransfection, the cells were observed under a microscope after Giemsa staining. (B) Expression of the MV envelope proteins on the cells. CHO/hSLAM cells were transfected with a plasmid expressing IC-H, SI-H, IC-F, or SI-F. The cells expressing IC-H (black line) and SI-H (gray line) were stained with an anti-H protein MAb (left panel), and the cells expressing IC-F (black line) and SI-F (gray line) were stained with an anti-F protein MAb (right panel). All the cells were subsequently stained with an Alexa Fluor 488-conjugated secondary antibody. The cells without transfection were stained with an anti-H protein MAb or an anti-F protein MAb followed by an Alexa Fluor 488-conjugated secondary antibody (shaded regions). (C) Diagrams of the chimeric F proteins. There are 10 amino acid differences (shown by vertical lines) between IC-F and SI-F. The regions derived from SI-F are shaded, and those derived from IC-F are white. The restriction enzyme-replaced fragments are indicated. (D) Syncytium formation in cells expressing the chimeric or mutant F proteins. CHO/hSLAM cells were transfected with a plasmid expressing IC-H together with plasmids expressing IC-F protein, SI-F protein, chimeric F protein (IC/SI-F-1, -F-2, -F-3, or -F-4), or mutant SI-F protein (G300E). At 24 h posttransfection, the cells were observed under a phase-contrast imaging microscope after Giemsa staining. (E) Quantification of syncytium formation. CHO/hSLAM cells were transfected with IC-H-expressing plasmids and IC-F-, SI-F-, chimeric F-, or mutant F-expressing plasmids together with an mCherry-expressing plasmid. At 48 h posttransfection, areas of each syncytium with mCherry autofluorescence were measured using an Axio Observer.D1 microscope and ImageJ software. Forty syncytia were measured for each F protein. Asterisks indicate that the area of syncytia induced by IC-F, chimeric F, or mutant F was significantly larger than that induced by SI-F, based on the results of a $t$ test ($P < 0.001$). The horizontal bars indicate the median values of the areas of syncytia.

teins) and nonstructural C and V proteins were well conserved in the SI strain (Table 1). We generated a recombinant MV possessing the IC323 genome in which the M, F, and H genes were replaced with those of the SI strain. The recombinant MV was designated IC/SI-MFH-AcGFP. The various types of cells shown in Fig. 4 were infected with IC/SI-MFH-AcGFP. IC/SI-MFH-AcGFP replicated poorly in SLAM- and ECR-positive cells and did not produce syncytia in these cells (Fig. 5A). A growth kinetics analysis of Vero/hSLAM cells, which were susceptible to all recombinant MVs, showed that IC/SI-MFH-AcGFP hardly produced cell-free viruses and exhibited a growth phenotype similar to that of SI-AcGFP (Fig. 4 and 5B). These data indicated that the membrane-associated protein-encoding genes (i.e., the M, F, and H genes) were responsible for the growth phenotype of the SI strain.

**The E300G substitution in the F protein is responsible for the reduced membrane fusion activity.** Previous papers have indicated that the typical changes in SSPE strains, namely, the lack of M protein expression and cytoplasmic tail truncation of the F protein, enhance the syncytium-forming activity of MV (6, 7). Indeed, other previous papers have shown high fusogenic activities of SSPE strains (1, 4, 8). Despite exhibiting the changes typical in SSPE strains, SI-AcGFP and IC/SI-MFH-AcGFP showed limited syncytium-forming activities (Fig. 4 and 5B). Using expression plasmids, the syncytium-forming activities of the H and F proteins of the SI strain were analyzed in CHO/hSLAM cells ($SLAM^+$). When the F protein of the SI strain (SI-F) was expressed together with the H protein of the SI strain (SI-H), no syncytia were detected (Fig. 6A; SI-H/SI-F). In contrast, many syncytia were observed when the F and H proteins of the IC-B strain (IC-F and IC-H, respectively) were expressed (Fig. 6A; IC-H/IC-F). Flow cytometry analyses indicated that the expression levels of SI-F and SI-H, respectively, were similar to those of IC-F and IC-H (Fig. 6B). The combination of SI-F and IC-H also showed poor syncytium-forming activity (Fig. 6A; IC-H/SI-F). On the other hand, when IC-F

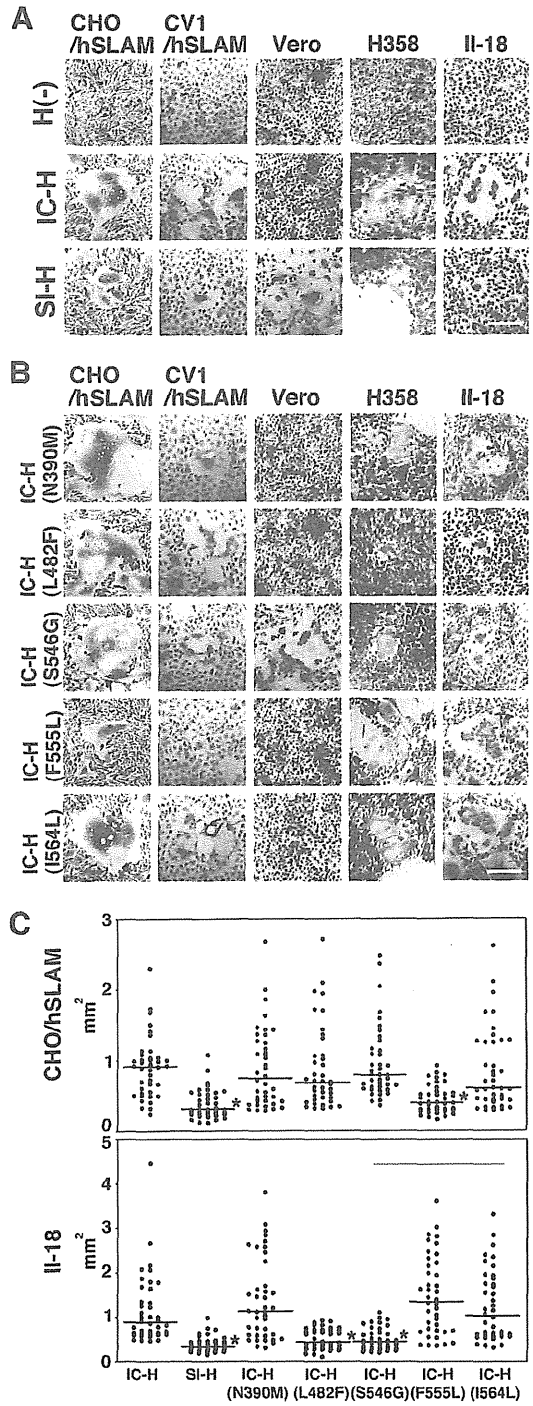


FIG. 7. Characterization of the amino acid residues in the SI-H protein that support cell-to-cell fusion in cells expressing SLAM, CD46, or ECR. (A and B) CHO/hSLAM, CV1/hSLAM, Vero, H358, and II-18 cells were transfected with plasmids expressing the H protein of the IC-B or SI strain (IC-H or SI-H, respectively) or no H protein [H(−)] (A) or mutant IC-H protein (N390M, L482F, S546G, F555L, or I564L) (B) together with a plasmid expressing the F protein of the IC-B strain. The CV1/hSLAM, H358, and II-18 cells were then incubated with an anti-CD46 MAb (M75). At 1 (CHO/hSLAM and CV1/hSLAM), 2 (Vero and II-18), or 3 (H358) days posttransfection, the cells were observed under a phase-contrast imaging microscope after Giemsa staining. Bars, 0.2 mm. (C) Quantification of syncytium formation. CHO/hSLAM and II-18 cells were transfected with IC-F-expressing plasmids and IC-H-, SI-H-, or mutant H-expressing plasmids together with an mCherry-expressing plasmid. At 48 h posttransfection, areas of each syncytium with mCherry autoflurescence were measured using an Axio Observer.D1 microscope and ImageJ software. Forty syncytia were measured for each H protein. Asterisks indicate that the area of syncytia induced by SI-H or mutant H was significantly smaller than that induced by the IC-H, based on the results of a *t* test ($P < 0.001$). The horizontal bars indicate the median values of the areas of syncytia.

was coexpressed with SI-H, many syncytia, albeit smaller in size than the syncytia induced by IC-F and IC-H, were detected (Fig. 6A; SI-H/IC-F). These data indicated that both the SI-F and SI-H proteins exhibited lower activities than the IC-F and IC-H proteins in inducing syncytia in CHO/hSLAM cells. To identify the mutation(s) that impaired the syncytium-forming activity of SI-F, four chimeric F proteins (IC/SI-F-1, -F-2, -F-3, and -F-4) were generated using the SI and IC-B strains (Fig. 6C). These chimeric F proteins were coexpressed with IC-H. Two chimeric F proteins, IC/SI-F-2 and IC/SI-F-4, failed to produce syncytia (Fig. 6D and E). These data showed that a region between the SalI and KpnI recognition sites (amino acid positions 271 and 324) in SI-F severely restricted its membrane fusion activity (Fig. 6C). In this region, only a single amino acid substitution, E300G, was found in comparisons of SI-F and IC-F (Fig. 6C and Table 2). A glycine residue at amino acid position 300 in SI-F was replaced with a glutamic acid. The mutant F protein [Fig. 6C; SI-F(G300E)] was expressed with IC-H. The data indicated that SI-F(G300E) caused membrane fusion as well as IC-F did ($P < 0.01$) [Fig. 6D and E; SI-F(G300E)]. These findings indicated that the SI-F protein exhibited a restricted membrane fusion activity that was mainly caused by the E300G substitution.

**S546G, L482F, and F555L substitutions affected the fusion-helper function of the H protein.** To analyze the fusion-helper function of SI-H in different cell types, the protein was expressed in CHO/hSLAM ($SLAM^+$), CV1/hSLAM ($SLAM^+$, $CD46^+$), Vero ($CD46^+$), H358 ($ECR^+$, $CD46^+$), and II-18 ($ECR^+$, $CD46^+$) cells together with IC-F. CD46-dependent infection was blocked by an anti-CD46 antibody (M75) when CV1/hSLAM, H358, and II-18 cells were used for the assessment of SLAM- and ECR-dependent infection. IC-H was used as a control. When IC-F was expressed alone, no syncytia were observed in either cell line [Fig. 7A; H(−)]. As reported previously, IC-H supported cell-to-cell fusion efficiently in SLAM-positive (CHO/hSLAM) and ECR-positive (H358 and II-18) cells but not in Vero cells (Fig. 7A; IC-H) (45, 49, 59). SI-H exhibited a fusion-helper function in Vero cells (Fig. 7A; SI-H), probably because of the S546G substitution. However, SI-H supported cell-to-cell fusion less efficiently than IC-H in CHO/hSLAM, CV1/hSLAM, H358, and II-18 cells (Fig. 7A; SI-H). To identify the substitution(s) responsible for the altered fusion-helper function of SI-H, five substitutions were individually introduced into IC-H and the mutated proteins were expressed in cells together with IC-F. The five selected substitutions were N390M, L482F, S546G, F555L, and 564L, since these substitutions were unique to the SI strain and

located in the receptor-binding globular head domain (Table 4). As expected, IC-H with S546G, but not the other mutant H proteins, supported cell-to-cell fusion in Vero cells (Fig. 7B). Instead, IC-H with S546G showed a reduced fusion-helper function in H358 and II-18 cells (Fig. 7B). No significant changes were observed in CHO/hSLAM and CV1/hSLAM cells after the introduction of the S546G substitution (Fig. 7B). Similarly, IC-H with L482F showed a reduced fusion-helper function in H358 and II-18 cells but showed activities similar to those seen with IC-H in CHO/hSLAM and CV1/hSLAM cells (Fig. 7B). Quantified and statistical analyses of cell-to-cell fusion in II-18 cells indicated that the areas of syncytia produced by IC-H(S546G) and IC-H(L482F) were significantly smaller than those produced by IC-H ($P < 0.01$) (Fig. 7C). None of the N390M, F555L, and I564L substitutions significantly affected the fusion-helper function in H358 and II-18 cells (Fig. 7B and C). These findings suggested that the L482F and S546G substitutions compromised the ability of the H protein to interact with ECR. It was also noted that the H protein with F555L showed a reduction in the fusion-helper function in CHO/hSLAM and CV1/hSLAM cells (Fig. 7B and C).

## DISCUSSION

SLAM is expressed on cells of the immune system and functions as the principal receptor for MV infection (69). However, this molecule probably plays a minor role in MV growth in the CNS, because neural cells in the brain do not express SLAM (28). Indeed, the ability of the SI strain to use SLAM was compromised by the F555L substitution. We and another group recently demonstrated that certain epithelial cells that form tight junctions are highly susceptible to MV infection (25, 50, 59). These data demonstrated the existence of ECR on some epithelial cells (25, 50, 59). ECR probably contributes to the efficient transmission of MV from a patient to other individuals (53), but its roles in persistent infection of the brain with MV remain to be elucidated. ECR is a candidate for an MV receptor in the brain. However, our data indicated that the SI strain had mutated via the S546G and L482F substitutions to use ECR inefficiently. With these data, the idea that ECR functions as a receptor for MV in the brain seemed unconvincing. Instead, the SI-H protein had adapted to use CD46 via the S546G substitution. Woelk et al. identified several positive-selection amino acid sites in the SSPE strain (67), but S546G was absent from the list. It is possible that the S546G substitution was introduced into the SI strain genome during the propagation in Vero cells but not in the brain, since the SI strain was isolated using Vero cells (29). Vero cells are 100 to 1,000 times less sensitive than SLAM-positive B95a cells for the isolation of wt MV strains (22, 34), and wt MV strains readily adapt to use CD46 after several passages in Vero cells (69). However, Ogura et al. (34) indicated that Vero cells were more sensitive than B95a cells for the isolation of SSPE strains. Although their data demonstrated that SSPE strains show cell specificities different from those of wt MV strains, some SSPE strains were shown not to use CD46 as a receptor (47). Nevertheless, it is still possible that the acquisition of the ability to use CD46 contributes to the growth of some SSPE-derived strains in the brain, since various SSPE strains may employ different strategies to acquire the ability to spread in the brain. The SI strain used only CD46 efficiently. Much evidence obtained using CD46-transgenic mice has shown the contributions of CD46 in establishing MV infection of the brain. Analyses using human brain samples also showed that CD46 is a candidate molecule that contributes to the growth of some SSPE strains in the brain (5, 28, 33).

Analyses using animal models have demonstrated that MV uses a transsynaptic route to spread between neurons (24, 27, 35, 40). The data indicated that receptors for the H protein are not required for the transsynaptic transmission (27, 70). It has been suggested that the F protein causes microfusion between neurons without the support of the H protein (27, 70). Ayata et al. (1) demonstrated that the F proteins of some SSPE strains contribute to the exhibition of neurovirulence in animals by showing a hyperfusion activity. Cattaneo et al. (4, 8) also demonstrated that the F proteins of SSPE strains exhibit higher levels of fusion activities than the standard F protein. These data suggest an important role for the F protein in the propagation of SSPE strains in the brain. However, our data indicated that the F protein of the SI strain showed limited membrane fusion activity because of the E300G substitution. It is unlikely that the F protein of the SI strain had acquired the E300G substitution during the propagation in cultured cells, since viruses usually acquire mutations that confer better fitness. Consequently, our data suggest that a high level of membrane fusion activity of the F protein was not a prerequisite for this SSPE strain to spread in the brain. Watanabe et al. (65) suggested that a reduction in cell-to-cell fusion mediated by amino acid changes in the F protein contributes to the persistence of MV in the brain. Their observations are consistent with our data for the SI strain. Thus, the data obtained in the present study provide a clear example of an SSPE-derived strain that exhibits limited fusion activity.

In the present study, we also established a reverse genetics system for the SI strain. Although we previously reported very efficient reverse genetics systems for MV, as shown using recombinant vaccinia viruses encoding T7 RNA polymerase (VV-T7) (30, 55, 56), they were not applicable for rescue of the SI strain from cloned cDNAs. When the previous systems were used (30, 56), infectious cycles of rSI-AcGFP were efficiently initiated in CHO/hSLAM cells by the use of the full-length genome plasmid (data not shown). However, since rSI-AcGFP did not produce cell-free virus particles and replicated poorly, it was impossible to isolate rSI-AcGFP from VV-T7. We tried to use a VV-T7-free system reported by Radecke et al. (39), but neither syncytia nor AcGFP fluorescence was detected. Therefore, a new, efficient VV-T7-free system was required for the rescue of rSI-AcGFP from cloned cDNAs. We are convinced that this new system used for the SI strain would be applicable for other SSPE strains. The success in establishing a reverse genetics system for an SSPE strain is a significant step toward the elucidation of the molecular bases and pathogenesis of SSPE.

## ACKNOWLEDGMENTS

We thank T. A. Sato and T. Seya for providing MAbs and N. Ito and M. Sugiyama for providing the BHK/T7-9 cells. We also thank K. Maenaka and all the members of Department of Virology 3, NIID, Japan, for technical help and suggestions.

This work was supported by grants from the Ministry of Education, Culture, Sports, Science and Technology and the Ministry of Health,

Labor and Welfare of Japan and a grant from The Uehara Memorial Foundation.

## REFERENCES


1. **Ayata, M., et al.** 2007. Effect of the alterations in the fusion protein of measles virus isolated from brains of patients with subacute sclerosing panencephalitis on syncytium formation. Virus Res. **130:**260–268.
2. **Baricevic, M., D. Forcic, M. Santak, and R. Mazuran.** 2007. A comparison of complete untranslated regions of measles virus genomes derived from wild-type viruses and SSPE brain tissues. Virus Genes **35:**17–27.
3. **Bellini, W. J., et al.** 2005. Subacute sclerosing panencephalitis: more cases of this fatal disease are prevented by measles immunization than was previously recognized. J. Infect. Dis. **192:**1686–1693.
4. **Billeter, M. A., et al.** 1994. Generation and properties of measles virus mutations typically associated with subacute sclerosing panencephalitis. Ann. N. Y. Acad. Sci. **724:**367–377.
5. **Buchholz, C. J., et al.** 1996. Selective expression of a subset of measles virus receptor-competent CD46 isoforms in human brain. Virology **217:**349–355.
6. **Cathomen, T., et al.** 1998. A matrix-less measles virus is infectious and elicits extensive cell fusion: consequences for propagation in the brain. EMBO J. **17:**3899–3908.
7. **Cathomen, T., H. Y. Naim, and R. Cattaneo.** 1998. Measles viruses with altered envelope protein cytoplasmic tails gain cell fusion competence. J. Virol. **72:**1224–1234.
8. **Cattaneo, R., and J. K. Rose.** 1993. Cell fusion by the envelope glycoproteins of persistent measles viruses which caused lethal human brain disease. J. Virol. **67:**1493–1502.
9. **Cattaneo, R., et al.** 1988. Biased hypermutation and other genetic changes in defective measles viruses in human brain infections. Cell **55:**255–265.
10. **Cattaneo, R., et al.** 1986. Accumulated measles virus mutations in a case of subacute sclerosing panencephalitis: interrupted matrix protein reading frame and transcription alteration. Virology **154:**97–107.
11. **Cattaneo, R., et al.** 1989. Mutated and hypermutated genes of persistent measles viruses which caused lethal human brain diseases. Virology **173:**415–425.
12. **Griffin, D. E.** 2007. Measles virus, p. 1551–1585. *In* D. M. Knipe et al. (ed.), Fields virology, 5th ed. Lippincott Williams & Wilkins, Philadelphia, PA.
13. **Grosfeld, H., M. G. Hill, and P. L. Collins.** 1995. RNA replication by respiratory syncytial virus (RSV) is directed by the N, P, and L proteins; transcription also occurs under these conditions but requires RSV superinfection for efficient synthesis of full-length mRNA. J. Virol. **69:**5677–5686.
14. **Hall, W. W., and P. W. Choppin.** 1979. Evidence for lack of synthesis of the M polypeptide of measles virus in brain cells in subacute sclerosing panencephalitis. Virology **99:**443–447.
15. **Hall, W. W., and P. W. Choppin.** 1981. Measles-virus proteins in the brain tissue of patients with subacute sclerosing panencephalitis: absence of the M protein. N. Engl. J. Med. **304:**1152–1155.
16. **Hall, W. W., R. A. Lamb, and P. W. Choppin.** 1979. Measles and subacute sclerosing panencephalitis virus proteins: lack of antibodies to the M protein in patients with subacute sclerosing panencephalitis. Proc. Natl. Acad. Sci. U. S. A. **76:**2047–2051.
17. **Halsey, N. A., et al.** 1980. Risk factors in subacute sclerosing panencephalitis: a case-control study. Am. J. Epidemiol. **111:**415–424.
18. **Hirano, A., A. H. Wang, A. F. Gombart, and T. C. Wong.** 1992. The matrix proteins of neurovirulent subacute sclerosing panencephalitis virus and its acute measles virus progenitor are functionally different. Proc. Natl. Acad. Sci. U. S. A. **89:**8745–8749.
19. **Ishida, H., et al.** 2004. Infection of different cell lines of neural origin with subacute sclerosing panencephalitis (SSPE) virus. Microbiol. Immunol. **48:** 277–287.
20. **Ito, N., et al.** 2003. Improved recovery of rabies virus from cloned cDNA using a vaccinia virus-free reverse genetics system. Microbiol. Immunol. **47:**613–617.
21. **Kato, A., et al.** 1996. Initiation of Sendai virus multiplication from transfected cDNA or RNA with negative or positive sense. Genes Cells **1:**569–579.
22. **Kobune, F., H. Sakata, and A. Sugiura.** 1990. Marmoset lymphoblastoid cells as a sensitive host for isolation of measles virus. J. Virol. **64:**700–705.
23. **Komase, K., et al.** 2006. The phosphoprotein of attenuated measles AIK-C vaccine strain contributes to its temperature-sensitive phenotype. Vaccine **24:**826–834.
24. **Lawrence, D. M., et al.** 2000. Measles virus spread between neurons requires cell contact but not CD46 expression, syncytium formation, or extracellular virus production. J. Virol. **74:**1908–1918.
25. **Leonard, V. H., et al.** 2008. Measles virus blind to its epithelial cell receptor remains virulent in rhesus monkeys but cannot cross the airway epithelium and is not shed. J. Clin. Invest. **118:**2448–2458.
26. **Leyrer, S., W. J. Neubert, and R. Sedlmeier.** 1998. Rapid and efficient recovery of Sendai virus from cDNA: factors influencing recombinant virus rescue. J. Virol. Methods **75:**47–58.
27. **Makhortova, N. R., et al.** 2007. Neurokinin-1 enables measles virus trans-synaptic spread in neurons. Virology **362:**235–244.
28. **McQuaid, S., and S. L. Cosby.** 2002. An immunohistochemical study of the distribution of the measles virus receptors, CD46 and SLAM, in normal human tissues and subacute sclerosing panencephalitis. Lab. Invest. **82:**403–409.
29. **Mirchamsy, H., et al.** 1978. Isolation and characterization of a defective measles virus from brain biopsies of three patients in Iran with subacute sclerosing panencephalitis. Intervirology **9:**106–118.
30. **Nakatsu, Y., M. Takeda, M. Kidokoro, M. Kohara, and Y. Yanagi.** 2006. Rescue system for measles virus from cloned cDNA driven by vaccinia virus Lister vaccine strain. J. Virol. Methods **137:**152–155.
31. **Ning, X., et al.** 2002. Alterations and diversity in the cytoplasmic tail of the fusion protein of subacute sclerosing panencephalitis virus strains isolated in Osaka, Japan. Virus Res. **86:**123–131.
32. **Niwa, H., K. Yamamura, and J. Miyazaki.** 1991. Efficient selection for high-expression transfectants with a novel eukaryotic vector. Gene **108:**193–199.
33. **Ogata, A., et al.** 1997. Absence of measles virus receptor (CD46) in lesions of subacute sclerosing panencephalitis brains. Acta Neuropathol. **94:**444–449.
34. **Ogura, H., et al.** 1997. Efficient isolation of subacute sclerosing panencephalitis virus from patient brains by reference to magnetic resonance and computed tomographic images. J. Neurovirol. **3:**304–309.
35. **Oldstone, M. B. A., et al.** 1999. Measles virus infection in a transgenic model: virus-induced immunosuppression and central nervous system disease. Cell **98:**629–640.
36. **Ono, N., et al.** 2001. Measles viruses on throat swabs from measles patients use signaling lymphocytic activation molecule (CDw150) but not CD46 as a cellular receptor. J. Virol. **75:**4399–4401.
37. **Parks, C. L., et al.** 2001. Comparison of predicted amino acid sequences of measles virus strains in the Edmonston vaccine lineage. J. Virol. **75:**910–920.
38. **Radecke, F., and M. A. Billeter.** 1995. Appendix: measles virus antigenome and protein consensus sequences. Curr. Top. Microbiol. Immunol. **191:**181–192.
39. **Radecke, F., et al.** 1995. Rescue of measles viruses from cloned DNA. EMBO J. **14:**5773–5784.
40. **Rall, G. F., et al.** 1997. A transgenic mouse model for measles virus infection of the brain. Proc. Natl. Acad. Sci. U. S. A. **94:**4659–4663.
41. **Richardson, C. D., A. Scheid, and P. W. Choppin.** 1980. Specific inhibition of paramyxovirus and myxovirus replication by oligopeptides with amino acid sequences similar to those at the N-termini of the F1 or HA2 viral polypeptides. Virology **105:**205–222.
42. **Sato, T. A., A. Fukuda, and A. Sugiura.** 1985. Characterization of major structural proteins of measles virus with monoclonal antibodies. J. Gen. Virol. **66:**1397–1409.
43. **Sato, T. A., M. Hayami, and K. Yamanouchi.** 1981. Antibody response to structural proteins of measles virus in patients with natural measles and subacute sclerosing panencephalitis. Jpn. J. Med. Sci. Biol. **34:**365–373.
44. **Schmid, A., et al.** 1992. Subacute sclerosing panencephalitis is typically characterized by alterations in the fusion protein cytoplasmic domain of the persisting measles virus. Virology **188:**910–915.
45. **Seki, F., M. Takeda, H. Minagawa, and Y. Yanagi.** 2006. Recombinant wild-type measles virus containing a single N481Y substitution in its haemagglutinin cannot use receptor CD46 as efficiently as that having the haemagglutinin of the Edmonston laboratory strain. J. Gen. Virol. **87:**1643–1648.
46. **Seya, T., et al.** 1995. Blocking measles virus infection with a recombinant soluble from of, or monoclonal antibodies against, membrane cofactor protein of complement (CD46). Immunology **84:**619–625.
47. **Shingai, M., et al.** 2003. Receptor use by vesicular stomatitis virus pseudotypes with glycoproteins of defective variants of measles virus isolated from brains of patients with subacute sclerosing panencephalitis. J. Gen. Virol. **84:**2133–2143.
48. **Shirogane, Y., et al.** 2008. Efficient multiplication of human metapneumovirus in Vero cells expressing the transmembrane serine protease TMPRSS2. J. Virol. **82:**8942–8946.
49. **Shirogane, Y., et al.** 2010. Epithelial-mesenchymal transition abolishes the susceptibility of polarized epithelial cell lines to measles virus. J. Biol. Chem. **285:**20882–20890.
50. **Tahara, M., et al.** 2008. Measles virus infects both polarized epithelial and immune cells by using distinctive receptor-binding sites on its hemagglutinin. J. Virol. **82:**4630–4637.
51. **Tahara, M., M. Takeda, and Y. Yanagi.** 2005. Contributions of matrix and large protein genes of the measles virus Edmonston strain to growth in cultured cells as revealed by recombinant viruses. J. Virol. **79:**15218–15225.
52. **Takasu, T., et al.** 2003. A continuing high incidence of subacute sclerosing panencephalitis (SSPE) in the Eastern Highlands of Papua New Guinea. Epidemiol. Infect. **131:**887–898.
53. **Takeda, M.** 2008. Measles virus breaks through epithelial cell barriers to achieve transmission. J. Clin. Invest. **118:**2386–2389.
54. **Takeda, M., et al.** 1998. Measles virus attenuation associated with transcriptional impediment and a few amino acid changes in the polymerase and accessory proteins. J. Virol. **72:**8690–8696.